國立交通大學

生物科技研究所

碩士論文

以定點突變改變 ***Arthrobacter globiformis*** 組織胺氧化酵素之受質特異性

Alteration of Substrate Specificity of *Arthrobacter globifomis* Histamine Oxidase by Site-Directed Mutagenesis

研 究 生：陳詩穎

指導教授：袁俊傑 博士

中 華 民 國 九 十 五 年 七 月

以定點突變改變 *Arthrobacter globiformis* 組織胺氧化酵素之

受質特異性

Alteration of Substrate Specificity of *Arthrobacter globifomis*

Histamine Oxidase by Site-Directed Mutagenesis

研 究 生：陳詩穎　　Student：Shih-Ying Chen

指導教授：袁俊傑 博士　　Advisor：Dr. Chiun-Jye Yuan

國 立 交 通 大 學

生 物 科 技 研 究 所

碩 士 論 文

A Thesis

Submitted to Department of Biological Science and Technology

National Chiao Tung University

in partial Fulfillment of the Requirements

for the Degree of

Master

in

Biological Science and Technology

July 2006

Hsinchu, Taiwan, Republic of China

中華民國九十五年七月

以定點突變改變 *Arthrobacter globiformis* 組織胺氧化酵素之

受質特異性

研 究 生：陳詩穎　　　　　　　　　指導教授：袁俊傑 博士

國立交通大學生物科技研究所碩士班

中文摘要

含銅胺類氧化酵素 [EC1.4.3.6] 廣泛存在於細菌、黴菌、酵母菌、植物及動物界。此類酵素大都以同源雙體的形式存在，其中每一單體包含一個銅離子及一個共價結合的 TPQ 輔因子，並藉由氧化脫胺作用分解一級胺類進而產生醛類，氨及過氧化氫。然而不同來源的胺類氧化酵素彼此之間的受質特異性具有很大的差異。為了釐清其中的影響因素，我們利用不同來源的胺類氧化酵素胺基酸序列比對和 QSAR 模型選出可能與受質特異性相關的胺基酸，分別是位在 AGHO 上 A156、P157、L158 這三個位置；之後依照 HPAO (*Hansenula Polymorpha* metylamine oxidase)的序列，產生突變株 A156D 與 A156D/L158W；且依照 BSAO (Bovin serum amine oxidase) 的序列，產生突變株 A156S/P157G/L158D、A156S/P157G、以及 L158D。實驗結果顯示所有的突變株皆具有正常的 TPQ 生成能力，但 A156D 與 A156D/L158W 的突變株具有較低甚至沒有酵素活性，推測原因可能是與 Leu 以 Trp 取代後造成的立體阻礙效應有關。而

突變株 A156S/P157G/L158D、A156S/P157G、及 L158D 對於 aromatic amines 的活性也是降低了；然而對於 aliphatic amines 的活性卻相對提升許多，尤其是 BSAO 的典型受質 spermine。因此，在我們的研究中說明了 A156、P157、以及 L158 可能扮演了與受質特異性有關的角色,並且成功地利用定點突變的方法改變了原有的受質特異性。

Alteration of Substrate Specificity of *Arthrobacter globifomis Histamine* Oxidase by Site-Directed Mutagenesis

Student：Shih-Ying Chen Advisor：Dr. Chiun-Jye Yuan

Department of Biological Science and Technology

National Chiao Tung University

Abstract

Arthrobacter globiformis histamine oxidase (AGHO) is a member of copper-containing amine oxidase (CAO) family [E.C. 1.4.3.6], which is ubiquitous distributed in bacteria, fungi, plants and animals. CAOs generally catalyze the oxidation of various primary amines to their corresponding aldehydes, with the subsequent release of ammonia and hydrogen peroxide. CAOs contain a topaquinone (TPQ) in their active site as the redox cofactor. Substrate preference of CAOs varies; while AGHO exhibits a broad spectrum of substrate specificity to aromatic primary amines. To investigate the important factors influencing its substrate specificity, a multiple sequences alignment, molecular modeling and small molecule docking and site-directed mutagenesis were employed. Upon multiple amino acid sequences alignment and molecular modeling and small molecule docking, three resides in AGHO, termed A156, P157, and L158, were studied due to their potential roles in substrate recognition, structure stability, and enzyme activity. Accordingly, A156D, A156D/L158W (mimic the active site residues of HPAO (*Hansenula Polymorpha* metylamine oxidase)), A156S/P157G and A156S/P157G/L158D (mimic active site residues of BSAO (Bovin serum amine oxidase)) were generated,

overexpressed and purified. We found the TPQ biogenesis was unaltered in these mutants. The catalytic activity of both A156D, A156D/L158W to aromatic amines was much lower than that of wild type, especially for A156D/L158W. It seems that, when Leu was changed to Trp, a steric effect may occur and hinder the access of substrate to the TPQ or cause an improper orientation of substrate directing to TPQ. Although, A156S/P157G/L158D, A156S/P157G, and L158D mutants also exhibit much lower catalytic activity to the aromatic amines than that of wild type AGHO, they show high catalytic activity to aliphatic amines, especially spermine, which is a typical substrate for BSAO. The results of this study suggest that A156, P157 and L158 play important roles in controlling the substrate specificity of AGHO and the replacement of these three amino acid residues may lead to conversion of substrate specificity of AGHO to the CAO from other species.

Acknowledgement

本論文能夠順利地完成，不單單只倚靠個人的辛苦以及努力，而是要歸功於許多人的指導、協助。在此，希望以我最誠摯的心意，向你們說聲「謝謝」。

首先感謝我的指導教授 袁俊傑老師，由於他不吝於分享其豐富的經驗與知識，讓我學會以更寬廣的角度去看事情、做實驗，耐心地傾聽我的想法、關心我的狀況，讓我的碩士生涯有了許多溫暖與陽光。亦感謝口試委員 楊裕雄老師與 梁勝富老師在口試時給予的寶貴意見，使得這篇論文更趨完善。

此外，也感謝研究室的許多伙伴們：學長姐俊炫、弘毅、威震、奕榮、佳穎、君璇、振剛、叔青、宜芳、元碩、岳縉給予我實驗上諸多的指導與協助，共患難的同學世昌、彥棋，學弟妹雯世、俊能、偉志的打氣與支持，因為你們，讓我的研究生涯更加充實與豐富。

還有我的好朋友們：含章、姿利、筱芳、惠珊、靖怡，因為有你們的友情支柱，讓我在面臨低潮沮喪時，總有力量克服困難。

最後，僅以此論文獻給我最愛的爸爸、媽媽、姊姊詩萍、哥哥思聖，謝謝你們不斷地付出、關懷，以及那份永無止盡的愛，讓我可以無後顧之憂地、恣意地享受自己所選擇的生活。這一路走來，心中充滿回憶與感謝，謝謝每一位曾經在我生命中的人。

Contents

Figure Contents

Table Contents

Appendix Contents

1. Introduction

Amine oxidases catalyze the oxidative deamination of amines to their corresponding aldehydes producing ammonia and hydrogen peroxide.

$$RCH_2NH_3^+ + O_2 + H_2O \longrightarrow RCHO + NH_4^+ + H_2O_2$$

Amine oxidases can be divided into two groups based on their cofactors, flavin-dependent monoamine oxidases (MAOs) and quinone-containing copper amine oxidases (CAOs). MAOs are found exclusively in the outer mitochondrial membrane of almost all cell types. These enzymes catalyze the oxidation of primary, secondary, and tertiary amines either by a concerted covalent catalysis or by a single electron-transfer mechanism, both requiring FAD as a cofactor [1]. CAOs generally catalyze the oxidation of primary amines through a ping-pong mechanism [2].

CAOs are widespread in nature, having been found in microorganisms, plants and animals [3-6]. They are involved in the oxidation of many short- and long-chain aliphatic monoamines and diamines, including several aromatic amines [3, 5]. In microorganisms, CAOs play a nutritional role that allows primary amines to be used as the source of carbon and nitrogen [3]. In higher organisms the physiological roles of CAOs are diverse and unclear so far. In plants, amine oxidases are though to aid in the biosynthesis of hormones, cell walls, and alkaloids [7, 8]. In mammals, the function of CAOs seems to be tissue specific involving physiological response to injury, apoptosis, cell growth, signaling, and detoxification [9, 10].

CAOs can be classified into two subfamilies based on the cofactors present in their active site. The 2, 4, 5-trihydroxyphenylalanine quinone (TPQ) is formed in a self-processing posttranslational modification of a conserved tyrosine within the sequence Ser/Thr-Xaa-Xaa-Asn-Tyr (TPQ)-Asp/Glu-Tyr/Asn. Molecular oxygen and copper are required in order for this modification to occur (Appendix 1) [11-13]. The second class of CAOs uses lysyl tyrosylquinone (LTQ) as their cofactor and is referred to as lysyl oxidase. Members of lysyl oxidases subfamily are involved in connective tissue maturation through the deamination of the side-chain of peptidyl lysine that initiate cross-linking of lysine residue in collagen and elastin [14].

The catalytic cycle of CAOs has been demonstrated by the cryocrystallography [15, 16]. In conjunction with single-crystal spectrophotometry and in trapping enzyme reaction intermediates, it provided detailed mechanistic information about the interaction of oxygen with a metalloenzyme (Appendix 2). The key step in catalysis is the conversion of the initial quinoneimine "substrate Schiff base" to a quinolaldimine "product Schiff base". This conversion is facilitated by a conserved aspartate residue, which act as a general base assisting proton abstraction from the α carbon of the substrate. Subsequently, the aldehyde product is released through hydrolysis. In the presence of O_2, oxidation to an iminoquinone species occurs, producing H_2O_2. The iminoquinone is then hydrolyzed, liberating NH^{4+} and returning the cofactor to its resting state. In addition, NH^{4+} may be released by a transimination reaction between the iminoquinine and substrate, thereby forming the "substrate

Schiff base" [17].

CAOs are homodimers, of which the molecular mass for each subunit is generally ranging from 70 to 100 kDa and contains variable carbohydrate content based on the origin of the enzymes. Currently, the crystal structures of several CAOs, ECAO (*Escherichia coli* amine oxidase; PDB code: 1OAC [18]), AGPEO (*Arthrobacter globiformis* phenylethylamine oxidase; PDB code: 1AV4; [3]), HPAO (*Hansenula polymorpha* amine oxidase; PDB code: 1A2V [19]), PPLO (lysyl oxidase from *Pichia pastoris*; PDB code: 1N9E [20]) , PSAO (CAOs from *Pisum sativum*; PDB code: 1KSI [21]), BSAO (CAOs from bovine plasma; PDB code: 1TU5 [22]), and hVAP-1 (human vascular adhesion protein; PDB code: 1US1 [23]). All of above CAOs share a similar 3D structure, even though they exhibit a low amino acid sequences identity of 25~35%.

Each subunit of the mushroom-shaped dimer comprises of three domains, named D2–D4; whereas in ECAO, there is one additional domain named D1 [18]. The D4 domain of each subunit binds tightly forming the interface of the dimer and part of the active site, which is highly conserved among species. The active site region of CAOs exhibits several similar structure features, a peptide-bound cofactor, TPQ or LTQ, a conserved catalytic aspartic acid residue and a copper ion for TPQ biogenesis. The active site of CAOs is a cavity that is deeply buried within each subunit and is accessible only via a channel formed by the D3 and D4 domains [23]. Besides, each monomer has a pair of α-hairpin arms, which extend from one subunit across the face of the other subunit. One of these arms partially defines the entrance to the active site channel in the other subunit and may play a role in substrate recognition [24]. This arm exhibits low amino acid homology among CAOs from different species. Differences in amino acid composition in this region provide unique characteristics to a given CAO in terms of the electrostatic properties, dimensions of the substrate channel, and the accessibility of substrates to TPQ [25].

Although the crystal structure of many CAOs have been solved, the fundamental questions, such as structure aspects of substrate specificity, the catalytic role of the copper ion, and possible cooperativity between the subunits, are still unresolved [2, 26]. The structural aspect of substrate specificity of CAOs is especially interesting to us and has been extensively studied by Yang in our laboratory [27]. In this study, the substrate preference of recombinant *Arthrobacter globiformi* histamine oxidase was investigated. Two copper amine oxidases, phenylethylamine oxidase (AGPEO) and histamine oxidase (AGHO), are released by Coryneform bacterium *A. globiformis*, when induced by phenylethylamine and histamine, respectively [28]. Despite the fact that the primary structures of two *A. globiformis* amine oxidases are similar, they share no immunochemical cross-reactivity [29]. The recombinant AGHO exhibits a substrate preference not only to histamine but also to other aromatic amines, such as phenylethylamine and tyramine. Upon molecular modeling, the active site pocket of AGHO is found to be surrounded by hydrophobic amino acid residues, suggesting that it prefers hydrophobic substrates. The K_{cat}/K_m value of AGHO to various substrates also increased with increase of the hydrophobicity of amines. Furthermore, the K_m value decreased in nearly linear fashion with increasing chain length of the alkyl carbon chain of aromatic amines [27]. However, factors that influence the substrate recognition of AGHO are still unknown. Therefore, it will be very interesting to understand factors that may influence the substrate specificity of AGHO.

In our current understanding, CAOs from different species exhibit diverse substrate specificities (Table 1) [16]. Only based on multiple amino acid sequences alignment of the channel from the different CAOs (Table 2), it's difficult to ascertain the previously described question. However, the molecular docking and quantitative structure activity relationships (QSAR) for AGHO are constructed [30]. The molecular docking tool QSAR is recently used in computer-aided drug design, and it is also helpful in this study to elucidate the possible binding status of amines in the active site cavity of AGHO. The QSAR was used to predict and verify the possible substrate of AGHO. In this case, benzylamine was predicted as the substrate of AGHO, and later was proved to be a poor substrate. By using QSAR model, we compress the correlative residues into F126, A156, P157, L158, Y316, D318, Y322, V399, N401 and F427 (Table 2).

Among the selected residues, D318, N401, Y316, and V399 of AGHO are highly conserved in all of the members of TPQ containing CAO subfamily. Other residues, such as F126, A156, P157, L158D, Y322, and F427, are variable in bacteria, yeasts, plants and animals, implying a role in substrate binding and recognition. The residue D318 has been indicated as the general base in the active site and N401 is important for the formation of TPQ [31]. AGPEO shows 61% identity to AGHO [29], of which similar structural features in the active site of

AGHO can be postulated. Molecular modeling and QSAR verification of AGHO based on known coordination of AGPEO has been done [30]. This allows us to predict the functions of certain residues in the active site of AGHO. Residue F126 of AGHO is related to F105 of AGPEO, A156 of AGHO is related to A135 of AGPEO, P157 of AGHO is related to P136 of AGPEO, L158 of AGHO is related to L137 of AGPEO, Y316 of AGHO is related to Y296 of AGPEO, Y322 of AGHO is related to Y302 of AGPEO, V399 of AGHO is related to L379 of AGPEO, and F427 of AGHO is related to F407 of AGPEO. The residue Y296 of AGPEO (Y316 in AGHO), for example, locates near the end of the substrate channel and acts as a "gate" to the active site. It appears to have an "open" conformation in all of the present AGPEO structures [32].

Based on the crystal structure of AGPEO [3], the active-site pocket and access channel are lined with many hydrophobic residues except Y302. The docking of an inhibitor, 4-(2-naphthyloxy)-2-butyn-1-amine, into the AGPEO active site as a Schiff base derivative was simulated and revealed that it made significant interactions with 5 residues, F105, W168, Y302, Y307, and W359 [25]. In these five residues, F105 and Y302 form π-stacking interactions with the inhibitor. Structural and kinetics studies of the interaction between AGPEO and 4-(aryloxy)-2-butynamines have provided further details of the active-site residues that may influence the substrate binding [17]. In the native structure, the peptide oxygen atom of P136 forms a hydrogen bond to a water molecule in the substrate access channel. Compared with the native structure, P136, which is close to F105, moves ~1.0Å (C^{γ}) to form a hydrogen bond from its peptide oxygen atom to the hydroxyl oxygen atom of Y302. The hydroxy group of Y302 also moves ~1 Å to form this new hydrogen bond. L137 also moves ($C^{\gamma 2}$ ~0.9 Å) thus avoiding a steric clash with the gate Y296 and the inhibitors. The side chain of I379 moves slightly ($C^{\gamma 2}$ ~1.3 Å) to a position where it is able to maintain hydrophobic packing with Y302, as well as to allow space for the product aldehyde ends of each inhibitor. The channel-blocking wire was used as an effective reversible CAO inhibitor to understand some of the structural subtleties that determine inhibitor potency. And it also reveals key aspects of active-site topology and conformational mobility. More importantly, the wire targets the active-site channel tracing the path of a substrate from the solvent to the active site [33]. This inhibitor is capable of making contacts of 3–5 Å with up to nine residues in the active-site channel and pocket. They are F105, A135, P136, L137, W168, Y296, Y302, G380, and F407.

In conclusion, we find three resides in AGHO, A156, P157, and L158, are interesting due to their potential in substrate recognition, structure stability, and enzyme activity. The amino acid sequence of this tripeptide (156-158) is highly homologous in CAOs from species within a kingdom; whereas it is less conserved across the kingdoms (Table 3). Accordingly, we generate a set of mutants, A156D, A156D/L158W, which mimic the tripeptide sequence of HPAO (*Hansenula Polymorpha* amine oxidase)). A set of mutants, L158D, A156S/P157G and A156S/P157G/L158D, which mimic tripeptide sequence of BSAO (bovine serum amine oxidase) were also generated. These mutants were overexpressed, purified and subjected to kinetics study. With these mutants, we hope to convert the substrate specificity of AGHO to that of HPAO and BASO.

We found that the TPQ biogenesis is unaltered in these mutants, but the mutants exhibit much lower catalytic activity to the aromatic amines than that of wild type AGHO. Despite no activity to small aliphatic amines, the mutant, A156D shows alterant activities; even A156D/L158W shows no activity toward to any amines. In regard to another set, all of these mutants show extremely high catalytic activity to physiological polyamines, which are typical substrates for BSAO. Above all, the mutant, A156S/P157G/L158D exhibits the obviously higher activity than the other two. It’s believed that the alteration of substrate recognition is mainly resulting from all of three sites mutated. The results of this study suggest that A156, P157 and L158 play important roles in controlling the substrate specificity of AGHO.

2. Materials and Methods

2-1. Materials

2-1-1. Vector and Expression System

Recombinant AGHO and AGHO^{mutants} genes were inert in plasmid pET30b without a S-tag (Appendix 3) in *E. coli* BL21(DE3).

2-1-2. Reagents

The chemicals were purchased from Merck and Sigma. Spectra/Por molecularporous membrane tubing was obtained from Spectrum Medical Industries, Inc. HiTrap-chelating column was purchased from Amersham Biosciences. Bradford's reagent was purchased from Bio-Rad. DNA Ladder and protein molecular weight marker were purchased from MBI. Prestained protein Ladder was purchased from Fermentas. Polyvinylidine diflutoide (PVDF) was obtained from Milllipore. All restriction enzymes were purchased from New England Biolabs, Inc. *Puf*Turbo DNA polymerase was purchased from Merck. All other reagents and chemicals used in the experiments were reagent grade.

2-2. Methods

2-1-1. Construction of Plasmids

The wild type AGHO in pUC-T and the expression vector pET30(-S)/AGHO was constructed previously in our laboratory [27, 34, 35]. The NotI fragment of wild type of AGHO gene (2069 bp) was purified from agarose gel and recovered using Gel/ PCR DNA Fragments Extraction Kit (GENEAID). The purified DNA fragment was then used to replaced the NotI fragement of AGHO gene in pET30(-S)/AGHO. The wild type AGHO in pGEM-T easy vector was constructed for the site-directed mutagenesis.

2-2-2. Site-Directed Mutagenesis

A156D, A156D/L158W, A156S/P157G, A156S/P157G/L158D, L158D mutants of AGHO were generated using QuickChange^{TM} Site-Directed Mutagenesis protocol (STRATAGENE) with pGEM-T easy/AGHO as a template. The reaction reagents contained 50 ng DNA templates, 125 ng forward and reverse primers, 2.5 U *Puf*Turbo DNA polymerase, and 0.5 mM dNTP in a final volume of 50 μL. The PCR condition was set following the protocol of manufacturer. Then add 10 U Dpn I restriction enzyme into the resulting PCR product to remove the original methylated template. The reaction was performed by incubating at 37 ℃ overnight. The Dpn I-treated PCR product (15 μL) was then transformed into DH5α competent cells and screened for mutants. Furthermore, the mutations of AGHO were confirmed by DNA sequencing.

2-2-3. E. coli Expression and Purification of AGHO and AGHO^{mutants}

The recombinant wild type AGHO and its mutants were overexpressd in *E. coli* BL21(DE3) cells carrying plasmid pET30b (-S). A single colony was picked from a freshly streaked plate (LB-agar, supplemented with 25 μg/mL kanamycin), incubated for 12 hours at 37 ℃, and then inoculated into 200 mL of LB medium. Flask cultures were grown at 37 ℃ and shacked at a speed of 150 rpm until the cell density reached A_{600nm} =0.4~0.6. Cells were induced with 50 μM isopropyl-1-thio-**β**-D-galactopyranoside (IPTG) and cultivated at 25 ℃ for 8 hours. Cells then were harvested by centrifugation at 6,000 rpm for 30 minutes.

The cell pellets were resuspended in 5 volumes of buffer A (50 mM potassium phosphate buffer, pH 6.8) and then disrupted on ice by ultrasonic disintegration with the sonic dismembrator (550, Fisher Scientific). The resulting lysates were centrifuged at 14,000 rpm for 30 minutes to remove insoluble particulates. The supernatants were first fractionated with ammonium sulfate (1-50%). The precipitates of 50% (w/w) ammonium sulfate were centrifuged at 10,000 rpm for 30 min and then dissolved in 1 mL buffer A. The resuscitations were dialyzed against buffer A at 4 ℃ for 12 hours and the buffer was renewed every 4 hours.

The protein solutions were then applied to a 1 mL pre-packed HiTrap-chelating column (Amersham Biosciences). The column was prepared following manufacturer's protocol. Briefly, the column was washed with 5 mL distilled water prior to the recharging of Ni ions by loading 1 mL Charge buffer (100 mM $NiSO_4$). Column was washed with 1 bed volume distilled water to remove the unbound metal ions. After column preparation, the column was equilibrated with 5 bed volumes of binding buffer (20 mM Tris-HCl, pH 7.9, 500 mM NaCl, 5 mM imidazole). Samples were centrifuged at 14,000 rpm for 15 min prior to loading on the column. Column was then washed with 10 bed volumes of binding buffer. To further remove non-specifically bound proteins the column can be washed with binding buffer containing 60 mM imidazole. The bound proteins were eluted with binding buffer containing 500 mM imidazole. Last but not least, the eluted protein was dialyzed overnight against buffer B (buffer A containing 50 μM $CuSO_4$) to allow the formation of metal-reconstituted proteins (including TPQ formation and Cu(II) binding). The unbound or weakly Cu(II) was removed from the protein by dialyzing with buffer A for 2~3 buffer changes (4 hours for each buffer change).

2-2-4. Protein Concentration Determination

Protein concentration was determined by Bradford protein assay (Bio-Rad) using bovine serum albumin as a standard. Briefly, the assay was performed in a constant reaction protocol by mixing 800 μL ddH_2O, 200 μL Bradford reagent, and 2 μL eluted protein solution. The mixture was vigorous vortexed and incubated under room temperature for 10 minutes. Determine the absorbance of mixture at wavelength 595 nm on the glass cuvette on a spectrophotometer (Hitachi U-3010). Calculate the protein concentration through intrapolation of a standard curve plotted on a same machine.

2-2-5. Activity Assay

Amine oxidase activity was determined spectrophotometrically by monitoring H_2O_2 production through a coupling assay by horseradish peroxidase (HRP) using DMAB (3-dimethyl-aminobenzoic acid) and MBTH (3-methyl-2-benzothiazolinone hydrazone) as substrates [36]. A DMAB-MBTH conjugated purple indamine dye formed during reaction can be measured at absorbance of 595 nm. Assays were carried out in 2 or 20 μg enzyme reaction with amine substrate in the detection buffer (2.5 U horseradish peroxidase, 2 mM DMAB, and 0.04 mM MBTH in 50 mM sodium phosphate buffer, pH 7.4) in a total volume of 1 mL at 30 °C for 5 minutes. Absorbance measurement was obtained with Hitachi U-3010 using quartz cuvettes with 1 cm path length. Calculate the value of enzyme activity through the slope plotted of UV Solutions 2.1 on the same mechanism. Blank assay medium did not contain substrates.

2-2-6. H_2O_2 Standard Curve

The procedure is the same as that of activity assay except that amine oxidase and substrates were replaced with H_2O_2 in amounts from 0.1 to 15 nmoles. The standard curve of H_2O_2 concentration and O.D. was illustrated in Figure 1.

2-2-7. Kinetic Measurement

Substrate stock solutions were freshly prepared in distilled water. The concentration of substrate in the kinetic study varies based on type of substrate due to substrate inhibition effect. The oxidation of substrates was determination by coupled assay (as described in ***Activity***

Assay). The data were fitted non-linearly by at least six or more substrate concentrations. The curve fitting was performed using Michaelis-Menten equation 1 on the SIGMA plot program Enzyme Kinetics Module 1.1.

$$V=Vmax / (1+Km/[S]) \quad (1)$$

And the substrates demonstrating substrate inhibition were using equation 2:

$$V=Vmax / (1+Km/[S] +[S]/Ki) \quad (2)$$

2-2-8. Electrophoresis and Redox-Cycling Staining

The protein solutions were separated on a 10% SDS polyacrylamide electrophoresis gel (SDS-PAGE). All SDS-PAGE was performed with a Bio-Rad Mini Protein II apparatus. Enzyme samples were boiled for 5 min in the presence of 100 mM dithiothreitol before loading onto the SDS-PAGE. The electrophoresis was performed at 100 Volt for 20 minutes first, followed at 140 Volt for another 1.5 hours. After electrophoresis, the gel was stained with 0.1% Coomassie Blue.

The redox-cycling approach provides a tool to reliably determine the quinone content of proteins for the study of the biological significance of this process and the factors that affect protein quinolation. The redox-cycling staining with NBT-Glycinate was determined as previous described [37]: the proteins were separated on 10% SDS-polyacryamide gels and transferred to a polyvinylidine difluroide (PVDF) membrane on a Bio-Rad Mini Trans-Blot Electrophoretic Transfer Cell soaked in an ice-cold transfer buffer (25 mM Tris, pH 8.3, 192 mM Glycine, 20% (v/v) methanol) at a constant current of 200 mA for 2 hours. After electro-blotting, the membrane was immersed in the Glycinate/NBT solution (0.24 mM Nitroblue Tetratzolium in 2 M potassium glycine, pH 10) for 30-45 minutes in the dark. The quinoproteins would be stained as blue-purple bands on the membrane.

3. Result and Discussion

3-1. The Construction of Mutants of AGHO and Expression of Wild Type and Mutants of AGHO

In this study, A156D, A156D/L158W, A156S/P157G, A156S/P157G/L158D, L158D mutants of AGHO were generated using QuickChange^{TM} Site-Directed Mutagenesis with pGEM-T easy/AGHO as a template. Then the pET-based bacterial expression system was chosen to express the wild-type and mutant of AGHO in E. coli. These proteins were cultivated in a copper-depleted medium and purified to homogeneity following protocol described by Yang in our laboratory [27]. As shown in Figure 2, the purity of wild type and mutants of AGHO was >99% as verified by SDS-PAGE.

3-2. Biogenesis of TPQ in AGHO Mutants

3-2-1. TPQ of Wild Type AGHO

The production of an active quinone-containing form of CAOs is dependent on the presence of Cu^{2+} ions. In previous study, we had demonstrated that the conversion of the precursor tyrosine to TPQ could be done in the presence of 50 μM $CuSO_4$ [27]. To reduce the oxidative damage of expressed recombinant protein by Cu(II), the enzyme was purified as an apo-form. Upon incubation with 50 μM $CuSO_4$ for overnight, the purified AGHO may exhibit a pale pink color suggesting the formation of TPQ; whereas the untreated, inactive enzyme (presumably an apo form) is colorless. To verify that TPQ does form in recombinant AGHO after Cu^{2+} treatment, the redox-cycling staning was employed. The cofactor TPQ has been shown to catalyze redox cycling under an alkaline pH with excess glycine as a reducting agent. In the presence of nitroblue tetrazolium and oxygen, tetrazolium is reduced to formazan and deposited onto the nitrocellulose membrane that contains recombinant AGHO (Figure 3). This result ensures that the TPQ is really formed in AGHO following the treatment of Cu^{2+}. After treatment, the unbound Cu(II) is removed by dialysis to ensure the maintenance of high enzyme activity for a long time.

3-2-2. TPQ formation of Mutants of AGHO

Similarly, all the mutants of AGHO used in this study were also purified as an apo form and then were converted to the holo form prior to the experiment. The formation of TPQ in the mutants of AGHO was verified by NBT/Glycine staining (Figure 4). This result reveals no obvious differences in the TPQ contents were observed among mutants and wild type AGHO, indicating that the formation of TPQ in these mutants is unaltered by the mutagenesis.

3-3. Study of Substrate Preference of Wild Type AGHO

Although histamine is reported to be the primary substrate for AGHO, other amines are also suggested to be catalyzed by this AGHO [38]. Therefore, the reactivity of active AGHO to various, natural, or xenobiotic amines (Appendix 4) were studied. The relative activities of AGHO to various amines (compared with histamine) at the concentration of 0.2 mM were calculated and listed in Table 4.

Accordingly, compared with histamine (100%), wild type AGHO exhibited higher reactivity to phenylethylamine (156.0 %) and tyramine (134.6 %). However, it exhibited 41.9 % and 23.9 % activity to phenylbutylamine and phenylpropylamine, respectively. AGHO shows a little or no activity to benzylamine (1.5%), cadverine (1.4 %), putrescine (0.7 %), and all the aliphatic amines studied.

Although CAOs exhibit common structural features, the substrate specificities of these enzymes appear to be different. Table 5 shows the kinetic constants (K_m, K_{cat}, K_{cat}/K_m) of wild type AGHO to various amines. Initial rate of AGHO at each concentration of corresponding amine substrate was determined at 30ºC within a time range of 0~5 minutes. The non-linear curve of initial rate vs. substrate concentration was fitted by an appropriate Michaelis-Menten equation (Eq.1 or Eq.2). The results show that almost all amines (except histamine and benzylamine) exhibit substrate inhibition to wild-type AGHO.

As shown in Table 5, the K_m value of wild type AGHO decreases when the alkyl carbon chain length that connects aromatic ring and the amino group of the aromatic amines increases from 1 to 4 carbons. The K_m value of AGHO for tyramine, which has one hydroxyl group on the aromatic ring, is slightly higher than that of phenylethylamine (Table 5). The values of k_{cat}/K_m, a representative of substrate specificity, are 0.054, 0.0013, 0.658, 0.385, 0.974, and 0.586 for histamine, benzylamine, phenylethylamine, phenylpropylamine, phenylbutylamine, and tyramine, respectively. The result indicates that phenylethylamine and its deverivatives are good substrates for wild type AGHO.

3-4. Studies of Substrate Preference of Mutants AGHO

3-4-1. Selection of Residues in AGHO for Site-Directed Mutagenesis

In our previous study, we have shown that AGHO prefer hydrophobic amines as its substrates [27]. The hydrophobicity is probably the determinant in substrate to affect its binding to AGHO, implying the presence of a lipophilic binding pocket at the active site of AGHO [3]. Thus, the hydrophobicity was used as an important factor to generate QSAR model of AGHO [30]. Based on the generated AGHO QSAR model, some amino acids residues, including F126, A156, P157, Y316, D318, Y322, V399, N401, and F427 are selected (Table 2). They are the consensus residues used in this study to evaluate the effect for QSAR modeling. Most of the selected residues are non-polar except Y316, D317, Y322, and N400. The multiple sequences alignment of CAOs (Table. 3) reveals that the residues Y316, D317, Y322, and N400 are either identical or highly conserved cross all five kingdoms. Interestingly, residues A156, P157, and L158 of AGHO are highly conserved within each kingdom; whereas the homology of these residues is low cross the kingdoms (Table 3). Thus, in this study, several single, double or triple mutants of AGHO was generated to mimic the active site residues of *Hansenula Polymorpha* amine oxidase (HPAO) (A156D and A156D/L158W) or bovine serum amine oxidase (BSAO) (L158D, A156S/P157G and A156S/P157G/L158D). Further kinetic studies will be performed.

3-4-2. Relative Activity and Kinetic studies of A156D mutant with

Various Substrates

The A156D mutant of AGHO was generated, overexpressed, and purified as demonstrated in Figure 2. The catalytic activity of A156D mutant toward various amines was much lower than those of wild type (Table. 4). The mutant exhibits a moderate to low reactivity to phenylethylamine (40.5 %), tyramine (23.5 %), histamine (18.9 %), phenylbutylamine (11.9 %), and phenylpropylamine (7.9 %). It shows nearly no activity to benzylamine (1.0%) and aliphatic amines.

Table 6 shows the kinetic parameters of A156D mutant. Compared with wild type AGHO, the K_m values of A156D to histamine, benzylamine, phenylethylamine and tyramine increased; whereas the k_{cat} values for the above amine were decreased (Table 10). Hence, the k_{cat}/K_m values for histamine, benzylamine, phenylethylamine and tyramine, were 0.004, 0.0002, 0.012 and 0.005, respectively, which were much lower than those of wild type AGHO (k_{cat}/K_m(histamine) = 0.054; k_{cat}/K_m(benzylamine) = 0.0013; k_{cat}/K_m(phenylethylamine) = 0.658; k_{cat}/K_m(tyramine) = 0.586). Different from wild type AGHO, no substrate inhibition was observed in A156D mutant, even the concentration of amines reached 1 mM. It was shown that the biogenesis of TPQ of this mutant was unaltered. Thus, A156 of AGHO may play a key role in mediating the catalysis of amines.

3-4-3. Relative Activity and Kinetic studies of A156D/L158W Mutant with Various Substrates

The double mutant of AGHO (A156D/L158W) was also generated, overexpressed, and purified (Figure 2). As shown in Table 3, A156D/L158W mutant shows no activity toward the amines studied. This result suggests that Leu 158 may be important in controlling the access of amines toward active site pocket. The molecular modeling of AGHO shows that Leu 158 lies in the proximity of substrate with its side chain closes to the ring of aromatic amines (Figure 5). When Leu was changed to Trp, a steric effect may be exerted by its bulk side chain. The bulk side chain of Trp may either hinder the access of substrate to the TPQ or cause the improper orientation of substrate directing to TPQ (Figure 6). In conclusion, A156 and L158 in AGHO may play important roles in controlling the binding and/or catalysis of substrates.

3-4-4. Relative Activity and Kinetic studies of A156S/P157G/L158D with Various Substrates

The A156S/P157G/L158D triple mutant of AGHO, which mimics the active site residues of BSAO (bovine serum amine oxidase), was generated, overexpressed, and purified (Figure 2). The substrate specificity of BSAO has been shown to prefer aliphatic amines, including putrescine, spermine, and spermidine [39-41]. In contrast, these aliphatic amines are neither substrates nor inhibitors of wild type AGHO. Therefore, the reactivity of this triple mutant toward putrescine and spermine will be studied. Different from wild type AGHO, A156S/P157G/L158D mutant has a low activity to aromatic amines, including tyramine (18.7 %), phenylbutylamine (16.1 %), phenylpropylamine (15.2 %), histamine (12.2 %), and phenylpropylamine (2.8 %) (Table 4). Interestingly, this triple mutant shows about 4.4~30-fold higher relative activity to aliphatic amines, including putrescine (8.3 %), cadcerine (6.2 %), spermine (6.1 %), spermidine (7.2 %), and norspermidine (7.5 %), than that of wild type AGHO (Table 4).

The K_m values of A156S/P157G/L158D triple mutant to histamine, phenylbutylamine, phenylpropylamine, phenylpropylamine and tyramine are similar; whereas the k_{cat} values to above aromatic amine reduced 50~95% (Table 11). Surprisingly, A156S/P157/L158D mutant exhibits a high affinity to spermine and putrescine with K_m values of 23.81 μM and 25.35 μM, respectively (Table 7). The k_{cat} values of the A156S/P157G/L158D mutant to spermine and putrescine are 0.32 s^{-1} and 0.29 s^{-1}, respectively. More interestingly, the K_m of BSAO to spermine is 20 μM [40]. This result suggests that the residues A156, P157, and L158 in AGHO are truly involved in the substrate recognition. The replacement of these residues with the active site sequence in BASO alters the substrate preference of AGHO from aromatic amine to aliphatic diamines, including putrescine and spermine. Compared with wild-type AGHO, the k_{cat}/K_m values of A156S/P156G/L158D mutant reduced 5~11-fold to histamine (0.009), benzylamine (0.006), phenylethylamine (0.074), phenylpropylamine (0.012), phenylbutylamine (0.352), and tyramine (0.044). Interestingly, the kinetic parameters for phenylbutylamine were not affected much by this mutagenesis with K_m and k_{cat} of 2.56 μM and 0.9 s^{-1}, respectively. A long butyl carbon chain may partially mimic the aliphatic amine that can be fitted into the active site of A156S/P157G/L158D mutant. A low substrate inhibition was observed on the A156S/P157G/L158D mutant with the K_i values of 344, 2248, 2402 and 2865 μM for phenylbutylamine, phenylethylamine, tyramine, and spermine, respectively.

3-4-5. Relative Activity and Kinetic studies of A156S/P157G with Various Substrates

A156S/P157G double mutant, partially mimic the active site residues of BSAO (bovine serum amine oxidase), was generated, overexpressed and purified (Figure 2). Compared with wild type AGHO, A156S/P157G exhibiteds normal reactivity to phenylethylamine (103.2 %) and tyramine (90.6 %), and moderate activity to histamine (64.4 %) and phenylbutylamine (60.4 %) (Table 4). Additionally, A156S/P157G shows a little or no activity to benzylamine (~1.0 %) and spermine. Interesting, the activity of A156S/P157G mutant toward diamine, such as putrescine, is higher than that of wild-type.

Table 8 displays the kinetic parameters of A156S/P157G mutant of AGHO to various substrates. Interestingly, substrate inhibition was not observed in A156S/P157G mutant. The K_m values for histamine, benzylamine, phenylethylamine and tyramine were higher than those of wild type AGHO (Table 12). However, the kinetic parameters of A156S/P157G mutant to phenylpropylamine, phenylbutylamine and spermine could not be determined in this study. The k_{cat}/K_m values of A156S/P157G mutant for histamine, benzylamine, phenylethylamine, tyramine and putrescine were lower than that of wild type AGHO and calculated as 0.020, 0.0004, 0.158, 0.181 and 0.0001, respectively. These results reveal that replacement of A156 and P157 to Ser and Gly, respectively, can induce its activity to putrescine, but may not be enough to turn the substrate specificity of AGHO from aromatic amines to aliphatic amines. Apparently, L158 may be important in determining the substrate selectivity of CAOs. However, A156 and P157 in AGHO may somewhat play roles mediating the substrate selectivity of the enzyme.

3-4-6. Relative Activity and Kinetic studies of L158D with Various Substrates

To understand the role of L158 in the substrate specificity of AGHO, a mutant L158D was generated, overexpressed and purified. As shown in Table 3, L158D mutant exhibited low activity to amines tested, including phenylethylamine (15.4 %), tyramine (11.8 %), phenylbutylamine (11.3 %), and histamine (5.0 %). L156D mutant shows little or no activity to phenylpropylamine (1.9 %), benzylamine (1.7 %), and aliphatic amines, including putrescine (4.0 %), cadcerine (3.1 %), spermine (1.1 %), spermidine (0.6 %), and norspermidine (0.5 %).

The K_m for histamine, phenylethylamine and tyramine was slight increased or decreased due to the mutation; whereas the K_m for benzylamine was largely decreased compared with that of wild-type AGHO (Table 14). For the aliphatic amines, including putrescine and spermine, the K_m values were 124.2 and 1830 μM, respectively, which were about 5- and 77-fold higher than that of A156S/P157G/L158D mutant (Table 15). However, the k_{cat} values of L156D mutant to putrescine and spermine were similar to that of A156S/P157G/L158D mutant. Several amines also exhibit substrate inhibition to L158D mutant, including benzylamine (574 μM), tyramine (744 μM), and phenylethylamine (1575 μM) (Table 9). Therefore, the single mutation of L158D also contributes to mediate the substrate binding and orientation in the active pocket.

Although L158D, A156S/P157G and A156S/P157G/L158D mutants can utilize putrescine and sperimine as substraes, only A156S/P157G/L158D mutant of AGHO mimic the substrate specificity of BSAO. Maybe when Pro was changed to Gly, the lack of β-carbon atom permits a substantially greater degree of conformational flexibility and attainable conformational space to admit long chains of amine. As for L158D, it's probably consistent with electrostatic attraction of positively charged substrates into the channel. Therefore there is a suitable circumstance driving the long chains and positively charged amino group of the substrate to the active site, in a correct orientation for the catalytic reaction (Figure 7). This result suggests that A156, P157 and L158 are essential in the active site of AGHO to mediate the substrate recognition and binding. The incomplete replacement of these three amino acid residues may lead to incomplete conversion of AGHO to BSAO in term of substrate specificity.

3-5. Future Application of AGHO

Although the reductive half-reaction and the reaction intermediates of the catalysis of AGHO have been well understoodl, the factors that influence the recognition and interaction between the substrate and the active site of CAOs are still unknown.

Since the substrates of AGHO are involved in numerous cellular functions, such as regulation of the synthesis of protein and nucleic acid, regulation of cell proliferation, differentiation and development, and involvement in detoxification and cell signaling processes. Based on the clinical investigation, SSAO have been detected under several pathophysiological conditions, particularly in diabetes mellitus, congestive heart failure and cirrhotic liver inflammation [42]. It has been suggested that some of the complications associated with diabetes, such as retinopathy, rephropathy, neuropathy, atherosclerosis and cardiovascular complications, may be caused by toxic products of SSAO-catalyzed reactions [43]. Therefore, CAOs have shown to be a potential target for anti-inflammatory drug screening. The inhibitors of CAOs may be used clinically to alleviate with diabetes.

Hence, knowledge of the factors controlling enzyme and substrate interactions can facilitate the design and optimization of selective agonist/antagonist. The results presented in this study may be helpful for the future application of AHGO mutants in fabrication of biosensors and drug screening.

Reference

1. Binda, C., A. Mattevi, and D.E. Edmondson, *Structure-function relationships in flavoenzyme-dependent amine oxidations: a comparison of polyamine oxidase and monoamine oxidase.* J Biol Chem, 2002. **277**(27): p. 23973-6.
2. Mure, M., S.A. Mills, and J.P. Klinman, *Catalytic mechanism of the topa quinone containing copper amine oxidases.* Biochemistry, 2002. **41**(30): p. 9269-78.
3. Wilce, M.C., et al., *Crystal structures of the copper-containing amine oxidase from Arthrobacter globiformis in the holo and apo forms: implications for the biogenesis of topaquinone.* Biochemistry, 1997. **36**(51): p. 16116-33.
4. Carter, S.R., et al., *Purification and active-site characterization of equine plasma amine oxidase.* J Inorg Biochem, 1994. **56**(2): p. 127-41.
5. Elmore, B.O., J.A. Bollinger, and D.M. Dooley, *Human kidney diamine oxidase: heterologous expression, purification, and characterization.* J Biol Inorg Chem, 2002. **7**(6): p. 565-79.
6. McGuirl, M.A., et al., *Purification and characterization of pea seedling amine oxidase for crystallization studies.* Plant Physiol, 1994. **106**(3): p. 1205-11.
7. McIntire, W., and Hartmann, C., *Copper-containing amine oxidases. In Principles and Applications of Quinoproteins.* Davidson, VL, Ed.; Marcel Dekker: New York, 1993: p. 97-172.
8. Sebela, M.F., I.; Petrivalsky, M.; Pec, P., *Copper/topa quinone-containing amine oxidases - recent research developments.* 2002. **26**: p. 1259-99.
9. Salmi, M., J. Hellman, and S. Jalkanen, *The role of two distinct endothelial molecules, vascular adhesion protein-1 and peripheral lymph node addressin, in the binding of lymphocyte subsets to human lymph nodes.* J Immunol, 1998. **160**(11): p. 5629-36.
10. Yu, P.H., et al., *Physiological and pathological implications of semicarbazide-sensitive amine oxidase.* Biochim Biophys Acta, 2003. **1647**(1-2): p. 193-9.
11. Ruggiero, C.E., et al., *Mechanistic studies of topa quinone biogenesis in phenylethylamine oxidase.* Biochemistry, 1997.

36(8): p. 1953-9.
12. Ruggiero, C.E. and D.M. Dooley, *Stoichiometry of the topa quinone biogenesis reaction in copper amine oxidases.* Biochemistry, 1999. **38**(10): p. 2892-8.
13. Prabhakar, R. and P.E. Siegbahn, *A theoretical study of the mechanism for the biogenesis of cofactor topaquinone in copper amine oxidases.* J Am Chem Soc, 2004. **126**(12): p. 3996-4006.
14. Wang, S.X., et al., *A crosslinked cofactor in lysyl oxidase: redox function for amino acid side chains.* Science, 1996. **273**(5278): p. 1078-84.
15. Wilmot, C.M., et al., *Visualization of dioxygen bound to copper during enzyme catalysis.* Science, 1999. **286**(5445): p. 1724-8.
16. Murray, J.M., et al., *Conserved tyrosine-369 in the active site of Escherichia coli copper amine oxidase is not essential.* Biochemistry, 2001. **40**(43): p. 12808-18.
17. O'Connell, K.M., et al., *Differential Inhibition of Six Copper Amine Oxidases by a Family of 4-(Aryloxy)-2-butynamines: Evidence for a New Mode of Inactivation.* Biochemistry, 2004. **43**(34): p. 10965-78.
18. Parsons, M.R., et al., *Crystal structure of a quinoenzyme: copper amine oxidase of Escherichia coli at 2 A resolution.* Structure, 1995. **3**(11): p. 1171-84.
19. Li, R., et al., *Crystallographic study of yeast copper amine oxidase.* Acta Crystallogr D Biol Crystallogr, 1997. **53**(Pt 4): p. 364-70.
20. Duff, A.P., et al., *The crystal structure of Pichia pastoris lysyl oxidase.* Biochemistry, 2003. **42**(51): p. 15148-57.
21. Kumar, V., et al., *Crystal structure of a eukaryotic (pea seedling) copper-containing amine oxidase at 2.2 A resolution.* Structure, 1996. **4**(8): p. 943-55.
22. Lunelli, M., et al., *Crystal structure of amine oxidase from bovine serum.* J Mol Biol, 2005. **346**(4): p. 991-1004.
23. Airenne, T.T., et al., *Crystal structure of the human vascular adhesion protein-1: unique structural features with functional implications.* Protein Sci, 2005. **14**(8): p. 1964-74.
24. Li, R., J.P. Klinman, and F.S. Mathews, *Copper amine oxidase from Hansenula polymorpha: the crystal structure determined at 2.4 A resolution reveals the active conformation.* Structure, 1998.

6(3): p. 293-307.
25. Shepard, E.M., et al., *Towards the development of selective amine oxidase inhibitors. Mechanism-based inhibition of six copper containing amine oxidases.* Eur J Biochem, 2002. **269**(15): p. 3645-58.
26. Mure, M., *Tyrosine-derived quinone cofactors.* Acc Chem Res, 2004. **37**(2): p. 131-9.
27. Yang, J.-G., *Research of Substrate Specificity of Arthrobacter globiformis Histamine Oxidase.*, in *institute of Biological Science and Technology* 2004, National Chiao Tung University.
28. Yoshida, S., et al., *Structure of rice-straw arabinoglucuronoxylan and specificity of Streptomyces xylanase toward the xylan.* Agric Biol Chem, 1990. **54**(2): p. 449-57.
29. Choi, Y.H., et al., *Copper/topa quinone-containing histamine oxidase from Arthrobacter globiformis. Molecular cloning and sequencing, overproduction of precursor enzyme, and generation of topa quinone cofactor.* J Biol Chem, 1995. **270**(9): p. 4712-20.
30. Chang, L.-J., *Integrating GEMDOCK with GEMPLS and GEMkNN for QSAR model of huAChE and AGHO.* , in *Institute of Bioinformatics* 2005, National Chiao Tung University.
31. Choi, Y.H., et al., *Role of conserved Asn-Tyr-Asp-Tyr sequence in bacterial copper/2,4, 5-trihydroxyphenylalanyl quinone-containing histamine oxidase.* J Biol Chem, 1996. **271**(37): p. 22598-603.
32. Kishishita, S., et al., *Role of copper ion in bacterial copper amine oxidase: spectroscopic and crystallographic studies of metal-substituted enzymes.* J Am Chem Soc, 2003. **125**(4): p. 1041-55.
33. Contakes, S.M., et al., *Reversible inhibition of copper amine oxidase activity by channel-blocking ruthenium(II) and rhenium(I) molecular wires.* Proc Natl Acad Sci U S A, 2005. **102**(38): p. 13451-6.
34. Chang, S.-P., *Characterization of Arthrobacter globiformis histamine oxidase by mutagenesis.*, in *institute of Biological Science and Technology*. 2003, National Chiao Tung University.
35. Lin, Y.-H., *Expression, mutagenesis and characterization of Arthrobacter globiformis amine oxidase I (histamine oxidase)*, in *institute of Biological Science and Technology*. 2002, National

Chiao Tung University.
36. Stoner, P., *An improved spectrophotometric assay for histamine and diamine oxidase (DAO) activity.* Agents Actions, 1985. **17**(1): p. 5-9.
37. Paz, M.A., et al., *Specific detection of quinoproteins by redox-cycling staining.* J Biol Chem, 1991. **266**(2): p. 689-92.
38. Shimizu, E., Odawara, T., Tanizawa, K., and Yorifuji, T., *Histamine oxidase, a quinoprotein enzyme of Arthrobacter globiformis*. Biosci. Biotech. Biochem., 1994. **58**: p. 2118-120.
39. Houen, G., et al., *Substrate specificity of the bovine serum amine oxidase and in situ characterisation of aminoaldehydes by NMR spectroscopy.* Bioorg Med Chem, 2005. **13**(11): p. 3783-96.
40. Di Paolo, M.L., et al., *Electrostatic compared with hydrophobic interactions between bovine serum amine oxidase and its substrates.* Biochem J, 2003. **371**(Pt 2): p. 549-56.
41. Lee, Y. and L.M. Sayre, *Reaffirmation that metabolism of polyamines by bovine plasma amine oxidase occurs strictly at the primary amino termini.* J Biol Chem, 1998. **273**(31): p. 19490-4.
42. Boomsma, F., et al., *Plasma semicarbazide-sensitive amine oxidase in human (patho)physiology.* Biochim Biophys Acta, 2003. **1647**(1-2): p. 48-54.
43. Gokturk, C., et al., *Overexpression of semicarbazide-sensitive amine oxidase in smooth muscle cells leads to an abnormal structure of the aortic elastic laminas.* Am J Pathol, 2003. **163**(5): p. 1921-8.
44. Cai, D. and J.P. Klinman, *Copper amine oxidase: heterologous expression, purification, and characterization of an active enzyme in Saccharomyces cerevisiae.* Biochemistry, 1994. **33**(24): p. 7647-53.
45. Tipping, A.J. and M.J. McPherson, *Cloning and molecular analysis of the pea seedling copper amine oxidase.* J Biol Chem, 1995. **270**(28): p. 16939-46.

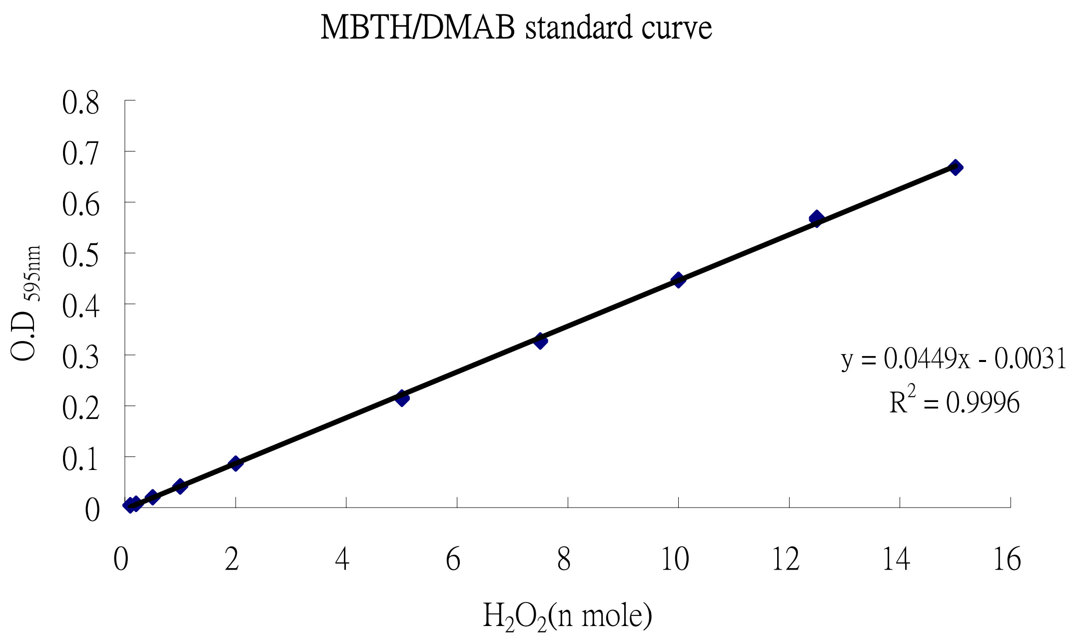

Figure 1. H_2O_2 standard curve.

The H_2O_2 standard curve was determined within the range between 0.1 to 15 nmole.

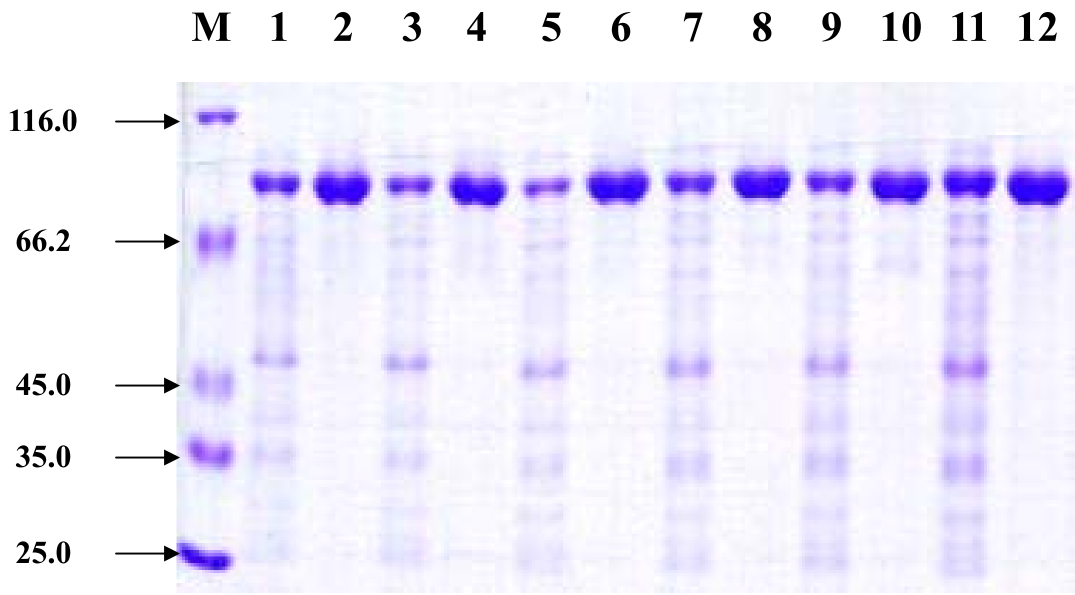

Figure 2. 10% SDS-PAGE of crude extract and purified wild type and AGHO mutants.

The crude extracts, purified wild-type AGHO, and AGHO mutants (all 3 μg) were separated on a 10 % SDS-PAGE and stained with Coomassie Blue. *M*: molecular weight standards (MBI Marker): 116.0, 66.2, 45.0, 35.0, and 25.0 kDa. *Lane 1,* crude extract containing Cu^{2+}-free apo form of AGHO; *Lane 2,* purified wild type AGHO; *Lane 3,* crude extract containing Cu^{2+}-free apo form of A156D mutant; *Lane 4,* purified A156D mutant; *Lane 5,* crude extract containing Cu^{2+}-free apo form of A156D/L158W mutant; *Lane 6,* purified A156D/L158W mutant; *Lane 7,* crude extract containing Cu^{2+}-free apo form of A156S/P157G mutant; *Lane 8,* purified A156S/P157G mutant; *Lane 9,* crude extract containing Cu^{2+}-free apo form of A156S/P157G/L158D mutant; *Lane 10,* purified A156S/P157G/L158D mutant; *Lane 11,* crude extract containing Cu^{2+}-free apo form of L158D mutant; *Lane 12,* purified L158D mutant.

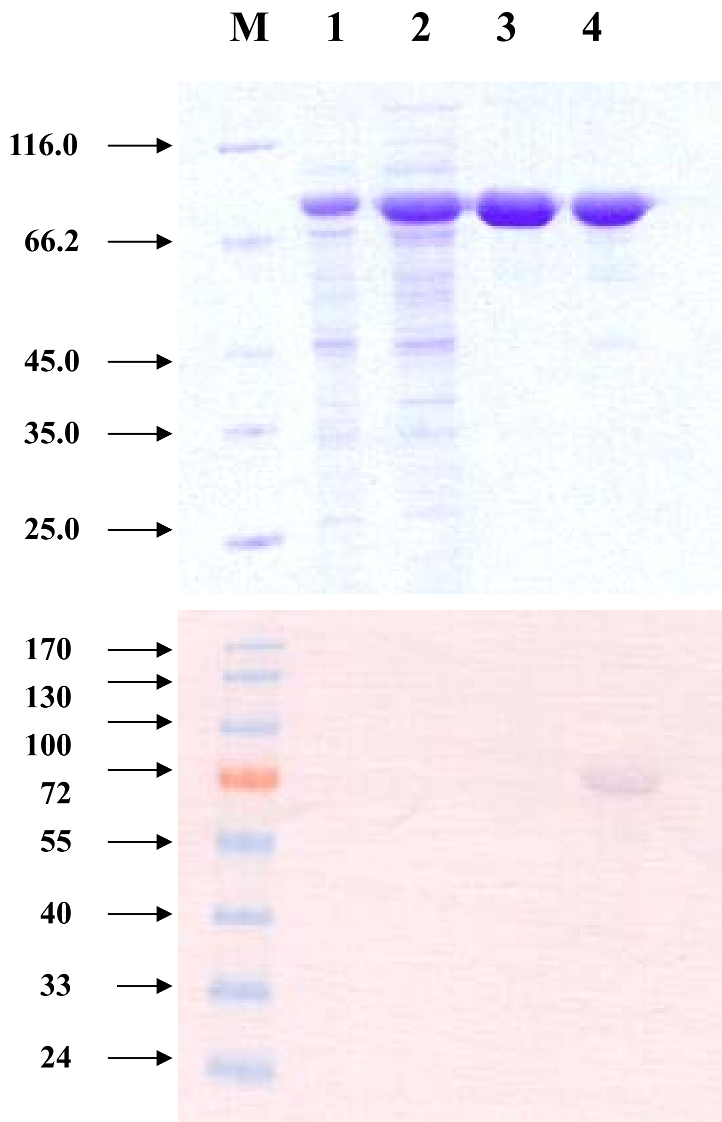

Figure 3. SDS-PAGE and NBT/Glycinate staining of wild type AGHO.

Crude extract (5 μg) containing wild type AGHO was loaded and separated on 10% SDS-PAGE. M: molecular weight Marker. *Lane 1,* crude extract; *Lane 2,* crude extract after ammonia sulfate (0-50%) of precipitation and dialyzed against buffer A; *Lane3,* Cu^{2+}-free inactive purified AGHO; *Lane 4,* Cu^{2+}-containing active AGHO.

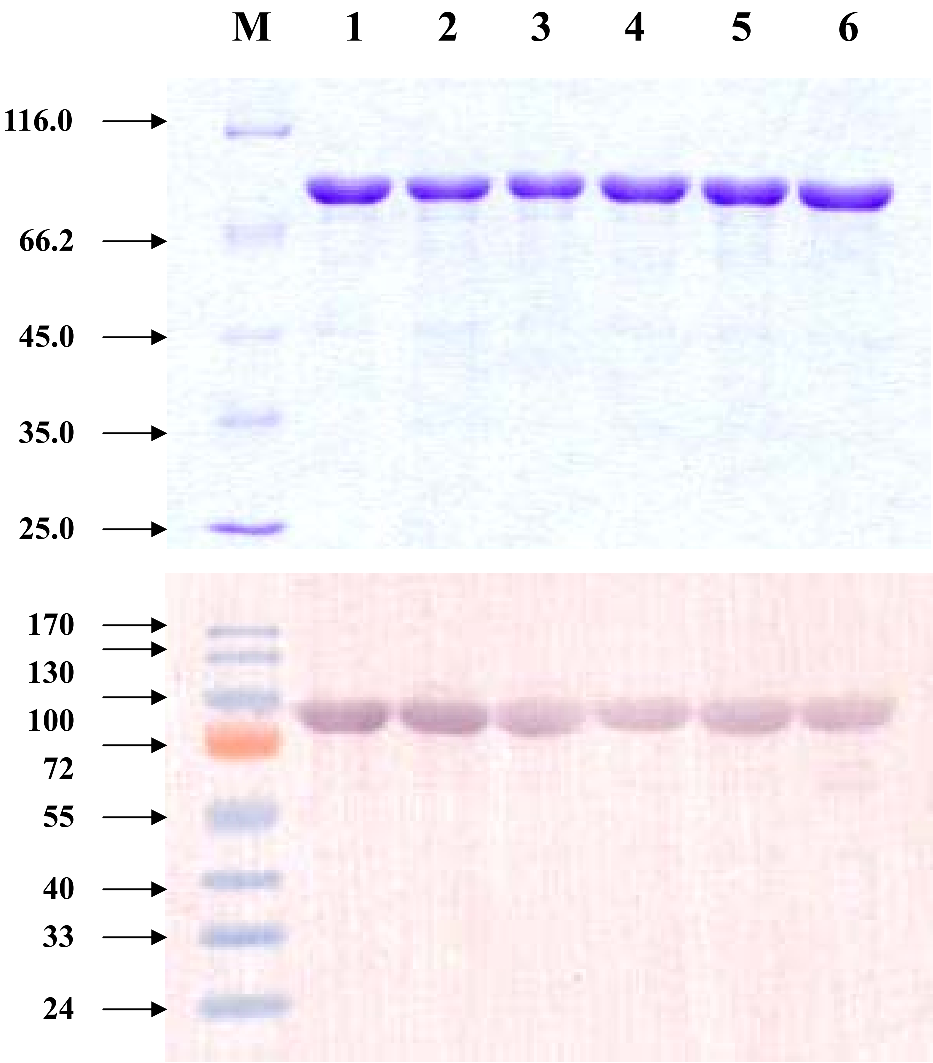

Figure 4. SDS-PAGE and NBT/Glycinate staining of purified wild type and AGHO mutants.

Purified protein (5 μg) was loaded and separated on 10% SDS-PAGE and subjected to Comassie blue staining (top panel) and NBT/glycinate staining (bottom panel). *Lane 1,* purified active form of wild type AGHO containing Cu^{2+}-containing active wild type AGHO. *Lane 2*: purified protein of Cu^{2+}; *Lane 3,* purified A156D/L158W mutant containing Cu^{2+}; *Lane 4,* purified A156S/P157G mutant containing Cu^{2+}; *Lane 5*: purified A156S/P157G/L158D mutant containing Cu^{2+}; *Lane 6,* purified L158D mutant containing Cu^{2+}.

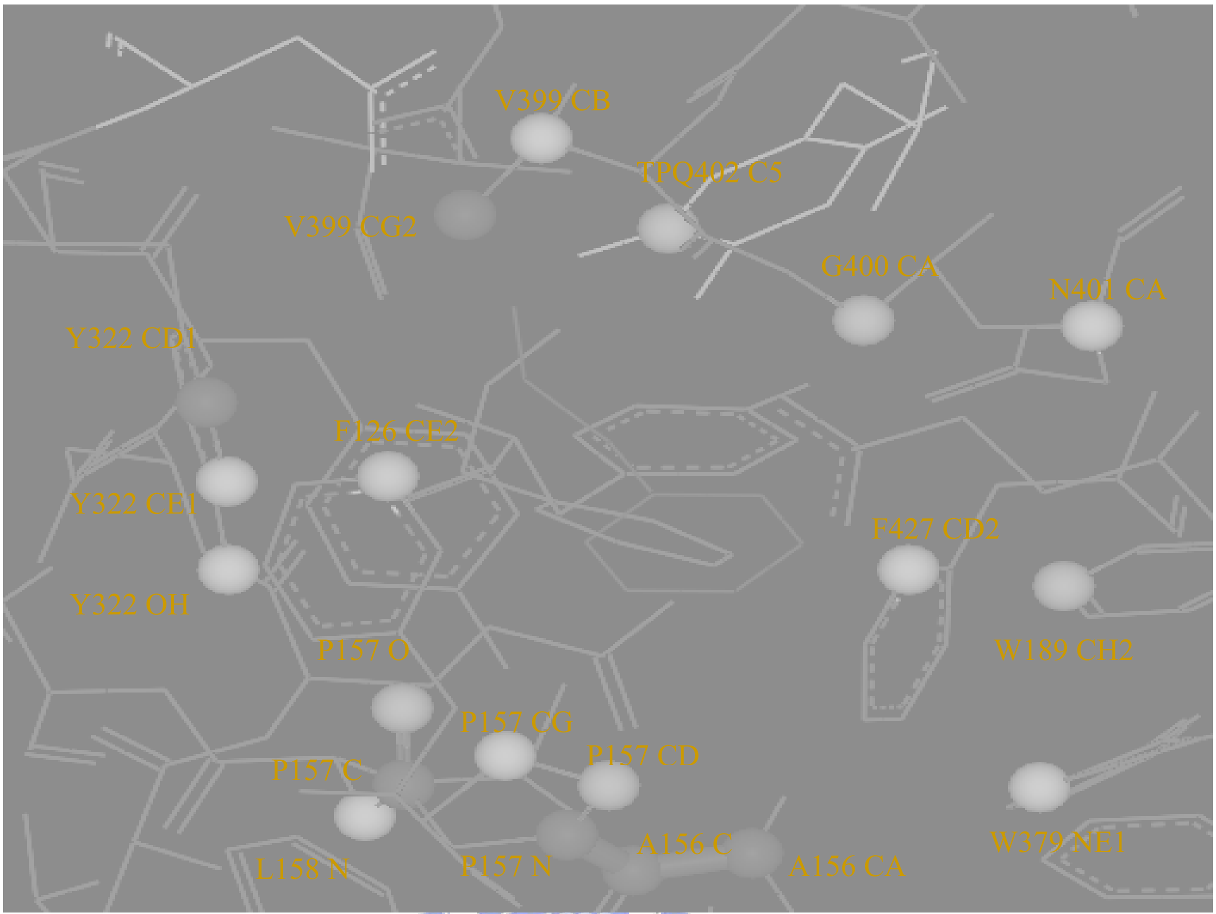

Figure 5. The predicted pose of phenylbutylamine at the active site of AGHO forms AGHO QSAR Model.

The residue number showed here is derived from the sequence of AGHO homology model.

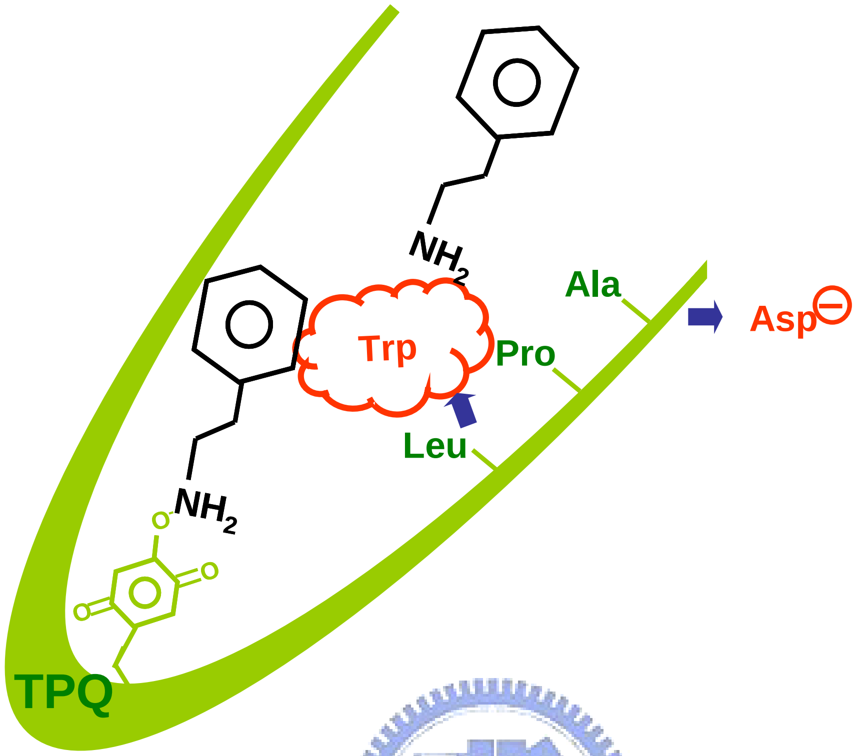

Figure 6. The proposed model for the binding of phenylethylamine in the active site of A156D/L158W mutant.

When Leu was changed to Trp, a steric effect may be exerted by its bulk side chain. The bulk structure of Trp can either hinder the access of substrate to the TPQ or cause the improper orientation of substrate directing to TPQ.

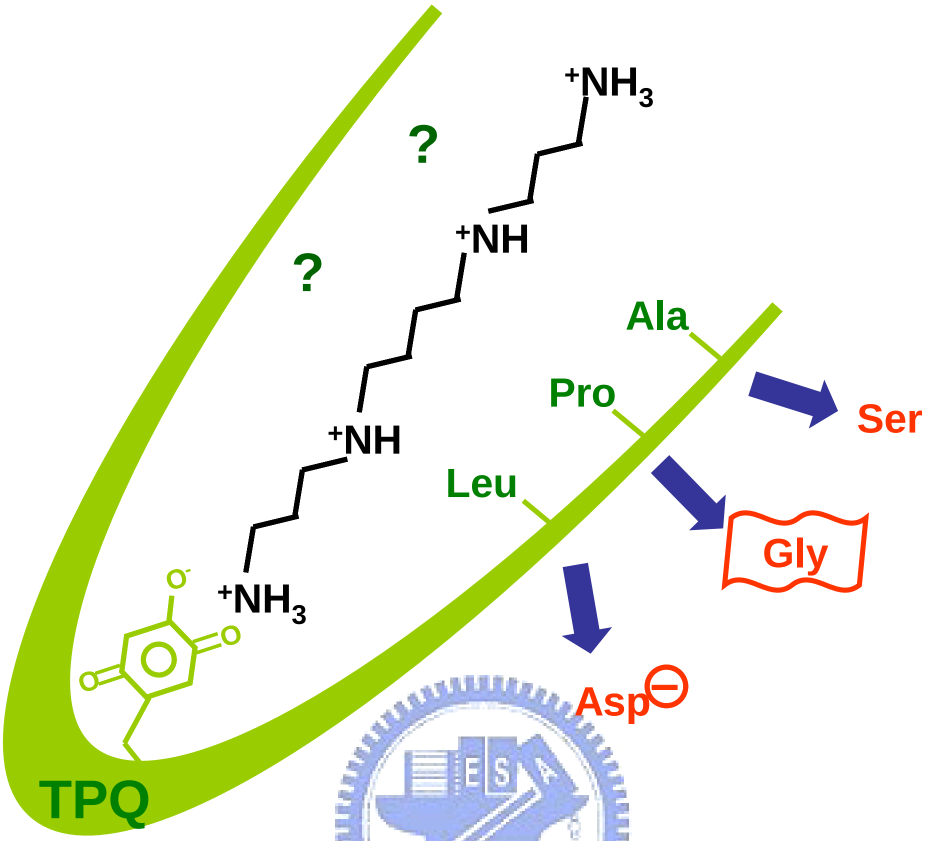

Figure 7. The proposed model for the binding of spermine in the active site of A156S/P157G/L158D mutant.

There is a suitable driving the long chains and positively charged amino group of the substrate to the active site, in a correct orientation for the catalytic reaction.

Table 1. CAOs are known to vary a great deal in their preferred substrate specificities.

The Source of Amine oxidase	Preferred Substrate
Kingdom Monera	Aromatic amine
e.g. AGPEO [3]	Phenylethylamine, Tyramine…
Kingdom Fungi	Small aliphatic amine
e.g. HPAO [24, 44]	Methylamine, Ethylamine…
Kingdom Plantae	Diamine
e.g. PSAO [45]	Putrescine, Cadaverine…
Kingdom Animalia	Long chains and hydrophobic character of amines
e.g. BSAO [39-41]	Spermidine, Spermine...

CAOs exhibit broad substrate specificity differences, depending on the different sources.

Table 2. The multiple sequences alignment of these residues of the channel from the different CAOs.

[a]Residues number is selected by AGHO QSAR model.

Residue number	123	124	126[a]	127	130	154	156[a]	157[a]	158	177	181	189	304	313	316[a]	318[a]	322[a]	327	377	378	379	398	399[a]	400	401[a]	402	427[a]
Kingdom Monera																											
AGHO	L	E	F	G	E	R	A	P	L	L	Q	W	Y	W	Y	D	Y	D	D	E	W	T	V	G	N	Y	F
AGPEO	E	E	F	E	E	R	A	P	L	L	Q	W	Y	W	Y	D	Y	Y	D	L	W	T	I	G	N	Y	F
ECAO	L	D	F	A	Q	I	T	P	L	I	D	W	Y	F	Y	D	Y	L	E	M	G	T	V	G	N	Y	A
KAMO	L	D	F	V	Q	V	T	P	L	V	D	W	Y	F	Y	D	Y	L	E	M	G	T	V	G	N	Y	A
Kingdom Fungi																											
ASNAO	L	T	S	E	T	V	E	P	W	L	T	Y	Y	R	A	D	G	M	N	W	R	T	L	A	N	Y	N
HPAO	V	E	L	C	E	Y	D	P	W	L	R	Y	Y	R	A	D	Y	M	D	F	R	T	A	A	N	Y	N
Kingdom Plantae																											
LSAO	S	A	E	Q	A	V	S	S	F	D	K	Y	Y	F	F	D	F	S	E	T	G	T	V	G	N	Y	E
PSAO	S	V	E	Q	A	V	S	S	F	D	K	Y	Y	F	F	D	F	S	E	N	G	T	V	G	N	Y	E
Kingdom Animalia																											
BSAO	L	R	Y	L	D	V	S	G	D	V	L	W	Y	L	Y	D	F	F	H	S	D	T	M	L	N	Y	S
hVAP-1	F	Q	Y	L	D	L	S	G	D	V	L	W	Y	T	Y	D	F	Y	H	S	D	T	L	L	N	Y	S
hABP	T	A	Y	A	Y	V	S	G	Q	T	L	W	Y	Q	Y	D	W	V	F	N	S	T	V	Y	N	Y	H

Table 3. The multiple sequences alignment of CAOs on the selected residues involved in substrate binding.

	Number of Amino Acids Involve in Substrate Binding									
CAO	126	156	157	158	316	318	322	399	401	427
AGHO	F	A	P	L	Y	D	Y	V	N	F
AGPEO	F	A	P	L	Y	D	Y	I	N	F
ECAO	F	T	P	L	Y	D	Y	V	N	A
KAMO	F	T	P	L	Y	D	Y	V	N	A
ASNAO	S	E	P	W	A	D	G	L	N	N
HPAO	L	D	P	W	A	D	Y	A	N	N
LSAO	E	S	S	F	F	D	F	V	N	E
PSAO	E	S	S	F	F	D	F	V	N	E
BSAO	Y	S	G	D	Y	D	F	M	N	S
hVAP-1	Y	S	G	D	Y	D	F	L	N	S
hABP	Y	S	G	Q	Y	D	W	V	N	H

The residue number showed in table is derived from the sequence of AGHO. It shows conserved in some special classes.

Table 4. Relative activity of wild type and mutant histamine oxidases

Relative activity (%)[a] of AGHO reacted with various substrates

Substrate	Wild	A156D	A156D /L158W	A156S /P157G /L158D	A156S /P157G	L158D
Histamine	100.0	18.9	-[b]	12.2	64.4	5.0
Benzylamine	1.5	1.0	-	2.4	1.0	1.7
Phenylethylamine	156.0	40.5	-	15.2	103.2	15.4
Phenylpropylamine	23.9	7.9	-	2.8	15.3	1.9
Phenylbutylamine	41.9	11.9	-	16.1	60.4	11.3
Tyramine	134.7	23.5	-	18.7	90.6	11.8
Methylamine	-	-	-	-	-	-
Ethylamine	-	-	-	-	-	-
Putrescine	0.7	0.4	-	8.3	1.4	4.0
Cadverine	1.4	0.7	-	6.2	1.8	3.1
Spermine	0.2	-	-	6.1	0.4	1.1
Spermidine	0.6	-	-	7.2	0.5	0.6
Norspermidine	0.3	-	-	7.5	0.5	0.5

[a]Relative substrate activities of selected amines (0.2 mM), in 50 mM phosphate buffer, pH 7.0.

[b]The negative symbol (-) denotes that substrate oxidation rate was too slow to determine it under our activity assay condition.

Table 5. Comparison of K_{cat}, K_{cat}/K_m, K_m, and K_i values toward wild type AGHO for various substrates

For Wild Type	K_m (μM)	K_{cat} (S^{-1})	K_i (μM)	K_{cat}/K_m ($\mu M^{-1}S^{-1}$)
Histamine	74.25 ± 9.19	3.99 ± 0.48	-	0.054
Benzylamine	36.22 ± 3.62	0.48 ± 0.01	-	0.0013
Phenylethylamine	8.07 ± 1.09	5.31 ± 0.12	648	0.658
Phenylpropylamine	3.43	1.32	309	0.385
Phenylbutylamine	2.55, 1.37 (1.96)[a]	1.82, 2.00 (1.91)	598, 641 (620)	0.974
Tyramine	8.56	5.02	1081	0.586
Putrescine	-	-	-	-
Spermine	-	-	-	-

[a]The value in bracket is the mean value.

Table 6. Comparison of K_{cat}, K_{cat}/K_m, K_m, and K_i values toward A156D mutant for various substrates

For A156D	K_m (μM)	K_{cat} (S^{-1})	K_i (μM)	K_{cat}/K_m ($\mu M^{-1}S^{-1}$)
Histamine	337.7 ± 61.4	1.40 ± 0.84	-	0.004
Benzylamine	246.8, 117.7 (182.3)	0.062, 0.17 (0.040)	-	0.0002
Phenylethylamine	198.9, 189.1 (194.0)	2.07, 2.59 (2.33)	-	0.012
Phenylpropylamine	-	-	-	-
Phenylbutylamine	-	-	-	-
Tyramine	170.8, 111.4 (141.1)	1.16, 0.40 (0.78)	-	0.005
Putrescine	-	-	-	-
Spermine	-	-	-	-

[a]The value in bracket is the mean value.

Table 7. Comparison of K_{cat}, K_{cat}/K_m, K_m, and K_i values toward A156S/P157G/L158D mutant for various substrates

For A156S/P157G/L158D	K_m (μM)	K_{cat} (S^{-1})	K_i (μM)	K_{cat}/K_m ($\mu M^{-1}S^{-1}$)
Histamine	35.84 ± 5.03	0.33 ± 0.11	-	0.009
Benzylamine	15.79, 10.45 (13.12)	0.074, 0.080 (0.077)	-	0.006
Phenylethylamine	5.38, 8.82 (7.10)	0.53, 0.52 (0.525)	2176, 2322 (2248)	0.074
Phenylpropylamine	5.22	0.064	-	0.012
Phenylbutylamine	2.56	0.90	344	0.352
Tyramine	12.53	0.55	2402	0.044
Putrescine	23.52, 27.18 (25.35)	0.26, 0.32 (0.29)	-	0.011
Spermine	21.89, 25.73 (23.81)	0.31. 0.32 (0.315)	2865	0.013

[a]The value in bracket is the mean value.

Table 8. Comparison of K_{cat}, K_{cat}/K_m, K_m, and K_i values toward A156S/P157G mutant for various substrates

For A156S/P157G	K_m (μM)	K_{cat} (S^{-1})	K_i (μM)	K_{cat}/K_m ($\mu M^{-1}S^{-1}$)
Histamine	110.1 ± 28.4	2.19 ± 0.53	-	0.020
Benzylamine	100.3	0.038	-	0.0004
Phenylethylamine	21.02	3.32	-	0.158
Phenylpropylamine	-	-	-	-
Phenylbutylamine	-	-	-	-
Tyramine	13.94	2.53	-	0.181
Putrescine	1567	0.23	-	0.0001
Spermine	-	-	-	-

[a]The value in bracket is the mean value.

Table 9. Comparison of K_{cat}, K_{cat}/K_m, K_m, and K_i values toward L158D mutant for various substrates

For L158D	K_m (μM)	K_{cat} (S^{-1})	K_i (μM)	K_{cat}/K_m ($\mu M^{-1}S^{-1}$)
Histamine	142.8, 154.74 (148.77)	0.29, 0.40 (0.35)	-	0.002
Benzylamine	5.35, 3.00 (4.14)	0.061, 0.065 (0.063)	574	0.015
Phenylethylamine	5.81, 5.08 (5.45)	0.54, 0.51 (0.52)	1575	0.095
Phenylpropylamine	-	-	-	-
Phenylbutylamine	-	-	-	-
Tyramine	13.92, 10.99 (12.46)	0.50, 0.42 (0.46)	744	0.037
Putrescine	148.5, 100.0 (124.2)	0.29, 0.25 (0.27)	-	0.002
Spermine	1830	0.36	-	0.0002

Table 10. Comparison of K_{cat}, K_{cat}/K_m, K_m, and K_i values toward wild type AGHO and A156D mutant

For Histamine	K_m (μM)	K_{cat} (S^{-1})	K_i (μM)	K_{cat}/K_m ($\mu M^{-1}S^{-1}$)
Wild Type	74.25	3.99	-	0.054
A156D	337.7	1.40	-	0.004

For Benzylamine	K_m (μM)	K_{cat} (S^{-1})	K_i (μM)	K_{cat}/K_m ($\mu M^{-1}S^{-1}$)
Wild Type	36.22	0.48	-	0.0013
A156D	182.3	0.04		0.0002

For Phenylethylamine	K_m (μM)	K_{cat} (S^{-1})	K_i (μM)	K_{cat}/K_m ($\mu M^{-1}S^{-1}$)
Wild Type	8.07	5.31	648	0.658
A156D	194	2.33	-	0.012

Table 10.　Continued

For Tyramine	K_m (μM)	K_{cat} (S^{-1})	K_i (μM)	K_{cat}/K_m ($\mu M^{-1}S^{-1}$)
Wild Type	8.56	5.02	1081	0.586
A156D	141.1	0.78	-	0.005

Table 11. Comparison of K_{cat}, K_{cat}/K_m, K_m, and K_i values toward wild type AGHO and A156S/P157G/L158D mutant

For Histamine	K_m (μM)	K_{cat} (S^{-1})	K_i (μM)	K_{cat}/K_m ($\mu M^{-1}S^{-1}$)
Wild Type	74.25	3.99	-	0.054
A156S/P157G/L158D	34.84	0.33	-	0.009

For Phenylethylamine	K_m (μM)	K_{cat} (S^{-1})	K_i (μM)	K_{cat}/K_m ($\mu M^{-1}S^{-1}$)
Wild Type	8.07	5.31	648	0.658
A156S/P157G/L158D	7.10	0.525	2248	0.074

For Tyramine	K_m (μM)	K_{cat} (S^{-1})	K_i (μM)	K_{cat}/K_m ($\mu M^{-1}S^{-1}$)
Wild Type	8.56	5.02	1081	0.586
A156S/P157G/L158D	12.53	0.55	2402	0.044

Table 11. Continued

For Phenylpropylamine	K_m (μM)	K_{cat} (S^{-1})	K_i (μM)	K_{cat}/K_m ($\mu M^{-1}S^{-1}$)
Wild Type	3.43	1.32	309	0.385
A156S/P157G/L158D	5.22	0.064	-	0.012

For Phenylbutylamine	K_m (μM)	K_{cat} (S^{-1})	K_i (μM)	K_{cat}/K_m ($\mu M^{-1}S^{-1}$)
Wild Type	1.96	1.91	620	0.974
A156S/P157G/L158D	2.56	0.9	344	0.352

Table 11. Continued

For Benzylamine	K_m (μM)	K_{cat} (S^{-1})	K_i (μM)	K_{cat}/K_m ($\mu M^{-1}S^{-1}$)
Wild Type	36.22	0.48	-	0.0013
A156S/P157G/L158D	13.12	0.077	-	0.006

For Putrescine	K_m (μM)	K_{cat} (S^{-1})	K_i (μM)	K_{cat}/K_m ($\mu M^{-1}S^{-1}$)
Wild Type	-	-	-	-
A156S/P157G/L158D	25.35	0.29	-	0.011

For Spermine	K_m (μM)	K_{cat} (S^{-1})	K_i (μM)	K_{cat}/K_m ($\mu M^{-1}S^{-1}$)
Wild Type	-	-	-	-
A156S/P157G/L158D	23.81	0.315	2865	0.013

Table 12. Comparison of K_{cat}, K_{cat}/K_m, K_m, and K_i values toward wild type AGHO, A156D mutant, and A156S/P157G mutant

For Histamine	K_m (μM)	K_{cat} (S^{-1})	K_i (μM)	K_{cat}/K_m ($\mu M^{-1}S^{-1}$)
Wild Type	74.25	3.99	-	0.054
A156D	337.7	1.40	-	0.004
A156S/P157G	110.1	2.19	-	0.020

For Benzylamine	K_m (μM)	K_{cat} (S^{-1})	K_i (μM)	K_{cat}/K_m ($\mu M^{-1}S^{-1}$)
Wild Type	36.22	0.48	-	0.0013
A156D	182.3	0.04		0.0002
A156S/P157G	100.3	0.038	-	0.0004

Table 12. Continued

For Phenylethylamine	K_m (μM)	K_{cat} (S^{-1})	K_i (μM)	K_{cat}/K_m ($\mu M^{-1}S^{-1}$)
Wild Type	8.07	5.31	648	0.658
A156D	194	2.33	-	0.012
A156S/P157G	21.02	3.32	-	0.158

For Tyramine	K_m (μM)	K_{cat} (S^{-1})	K_i (μM)	K_{cat}/K_m ($\mu M^{-1}S^{-1}$)
Wild Type	8.56	5.02	1081	0.586
A156D	141.1	0.78	-	0.005
A156S/P157G	13.94	2.53	-	0.181

Table 13. Comparison of K_{cat}, K_{cat}/K_m, K_m, and K_i values toward wild type AGHO, A156S/P157G/L158D mutant, and A156S/P157G mutant

For Putrescine	K_m (μM)	K_{cat} (S^{-1})	K_i (μM)	K_{cat}/K_m ($\mu M^{-1}S^{-1}$)
Wild Type	-	-	-	-
A156S/P157G/L158D	25.35	0.29	-	0.011
A156S/P157G	1567	0.23	-	0.0001

For Spermine	K_m (μM)	K_{cat} (S^{-1})	K_i (μM)	K_{cat}/K_m ($\mu M^{-1}S^{-1}$)
Wild Type	-	-	-	-
A156S/P157G/L158D	23.81	0.315	2865	0.013
A156S/P157G	-	-	-	-

Table 14. Comparison of K_{cat}, K_{cat}/K_m, K_m, and K_i values toward wild type AGHO and L158D mutant

For Histamine	K_m (μM)	K_{cat} (S^{-1})	K_i (μM)	K_{cat}/K_m ($μM^{-1}S^{-1}$)
Wild Type	74.25	3.99	-	0.054
L158D	142.8	154.74	-	0.002

For Phenylethylamine	K_m (μM)	K_{cat} (S^{-1})	K_i (μM)	K_{cat}/K_m ($μM^{-1}S^{-1}$)
Wild Type	8.07	5.31	648	0.658
L158D	5.45	0.52	1575	0.095

For Tyramine	K_m (μM)	K_{cat} (S^{-1})	K_i (μM)	K_{cat}/K_m ($μM^{-1}S^{-1}$)
Wild Type	8.56	5.02	1081	0.586
L158D	12.46	0.46	744	0.037

Table 15. Comparison of K_{cat}, K_{cat}/K_m, K_m, and K_i values toward wild type AGHO, A156S/P157G/L158D, and L158D mutant

For Benzylamine	K_m (μM)	K_{cat} (S^{-1})	K_i (μM)	K_{cat}/K_m ($\mu M^{-1}S^{-1}$)
Wild Type	36.22	0.48	-	0.0013
A156S/P157G/L158D	13.12	0.077	-	0.006
L158D	4.14	0.063	574	0.015

For Putrescine	K_m (μM)	K_{cat} (S^{-1})	K_i (μM)	K_{cat}/K_m ($\mu M^{-1}S^{-1}$)
Wild Type	-	-	-	-
A156S/P157G/L158D	25.35	0.29	-	0.011
L158D	124.2	0.27	-	0.002

Table 15. Continued

For Spermine	K_m (μM)	K_{cat} (S^{-1})	K_i (μM)	K_{cat}/K_m ($\mu M^{-1}S^{-1}$)
Wild Type	-	-	-	-
A156S/P157G/L158D	23.81	0.315	2865	0.013
L158D	1830	0.36	-	0.0002

Appendix 1. Mechanism for the biogenesis of TPQ in CAOs

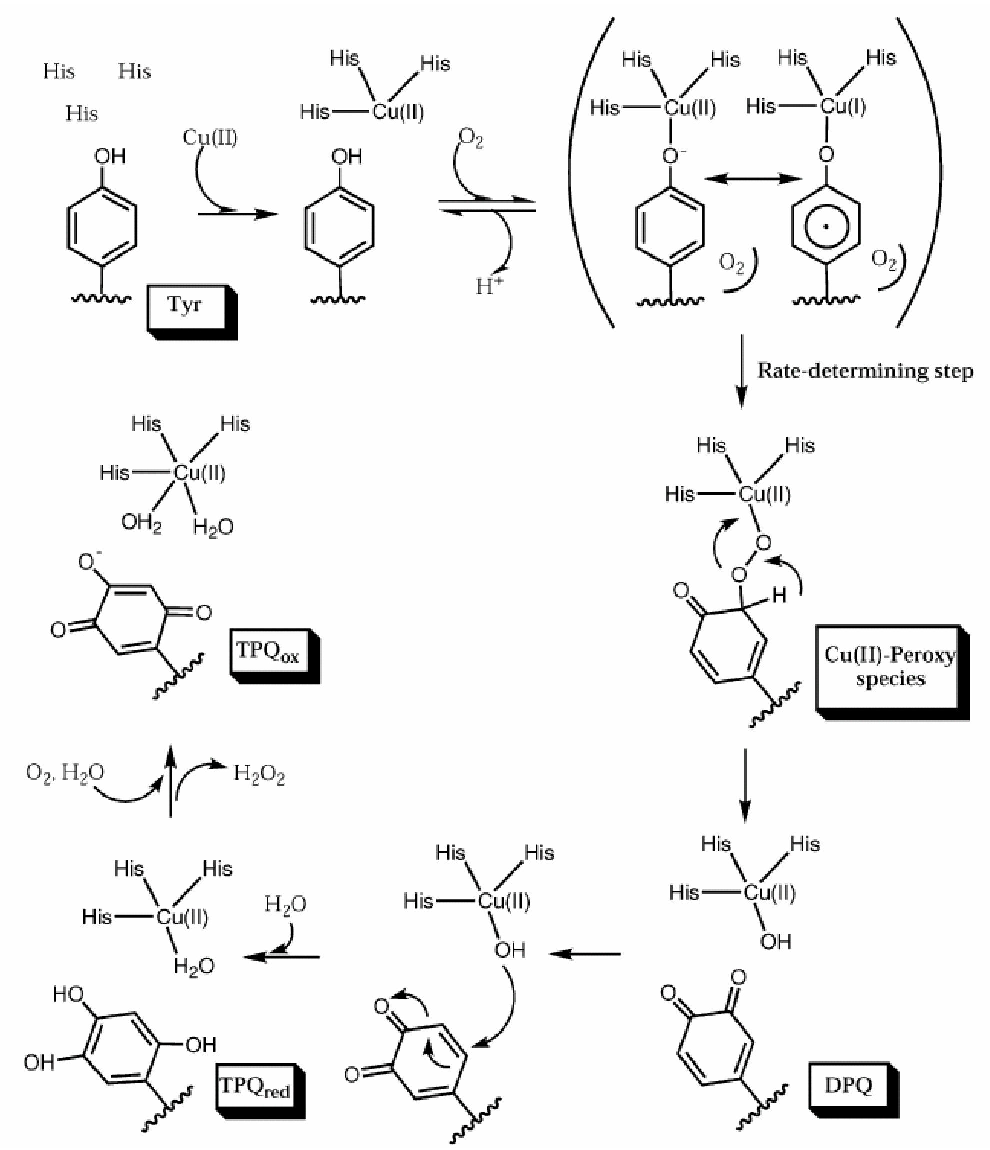

The mechanism is divided into six steps. At first, copper binds anaerobically to the enzyme (step 1). Second, dioxygen binds at a site near the precursor tyrosine (step 2) and is proposed to react with the Cu (II)-tyrosinate species and form a bridging peroxy intermediate (step 3). Then the DPQ ring first rotates 180° around the Cβ-Cγ bond so that the C-2 position of TPQ facesthe Cu metal center (step 4). The C-2 site of TPQ is oxidized (step 5). In the final step of the mechanism, dioxygen enters, and hydrogen peroxide is formed (step 6) [13].

Appendix 2. Pathway for the catalytic cycle

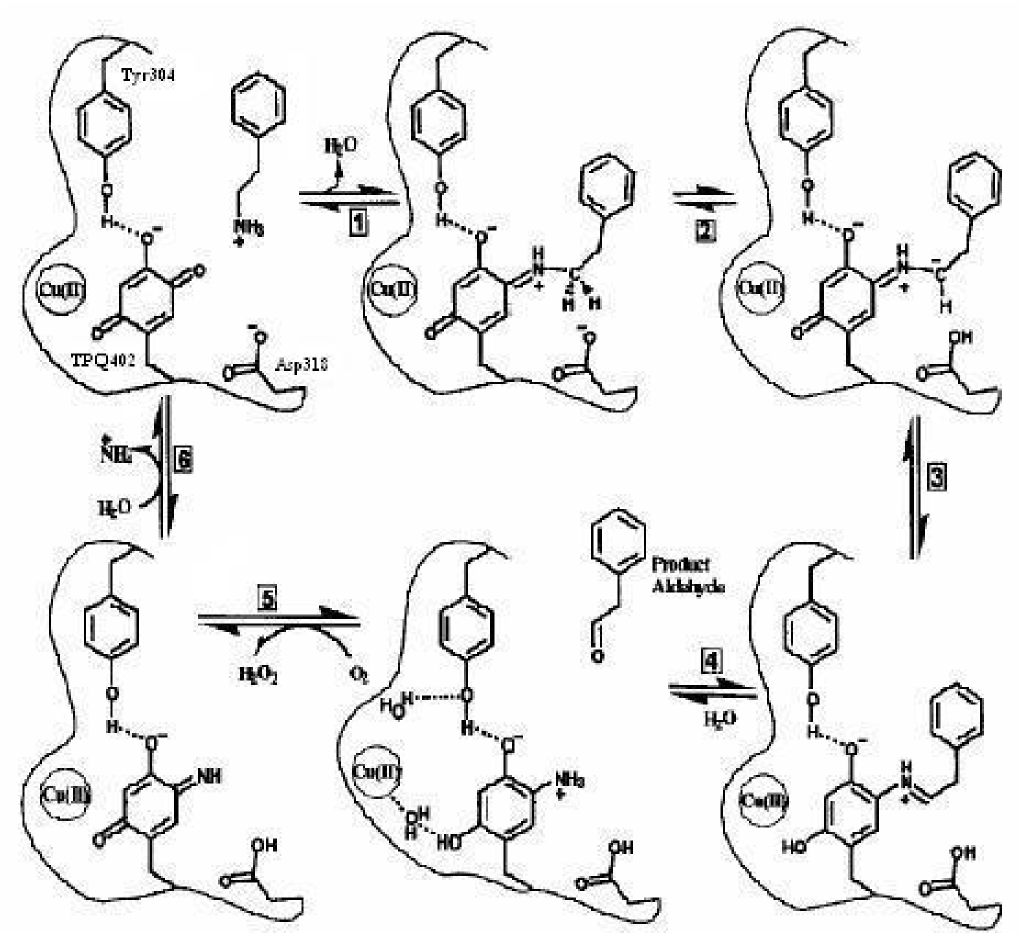

The TPQ is shown together with the active site base, Asp318, and the conserved Tyr304. The substrate is deprotonated and forms the substrate Schiff base (step 1). A hydrogen is abstracted, by Asp318, from the methylene group (step 2), allowing rearrangement to the product Schiff base (step 3). Product aldehyde is released by hydrolysis to leave reduced enzyme (step 4); some hydrogen bonds associated with the reduced (aminoquinol) TPQ are shown by dashed lines. Oxygen, the second substrate, binds to the enzyme and is reduced to hydrogen peroxide (step 5), giving iminoquinone with subsequent hydrolysis and release of ammonia, regenerating the active enzyme (step 6) [16].

Appendix 3. Plasmid map of pET30b(-S)/AGHO

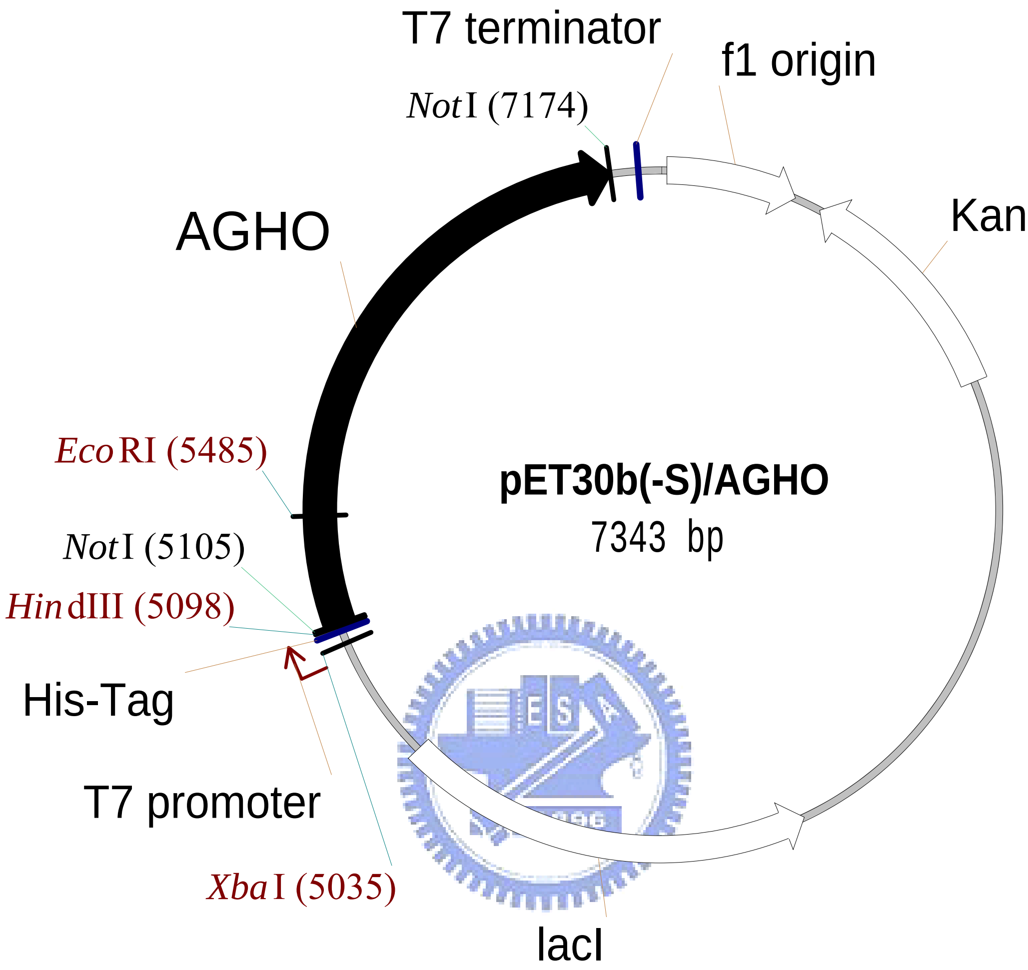

Appendix 4.   Amine list

Aliphatic amine

Chemical Name Molecular Formula	Synonyms	Structural Formula
Methylamine CH_5N	Aminomethane; Methanamine; Monomethylamine	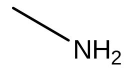
Ethylamine C_2H_7N	Aminoethane; Ethanamine; Monoethylamine	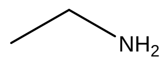
1,4-Diaminobutane $C_4H_{12}N_2$	1,4-Butanediamine; Putrescine	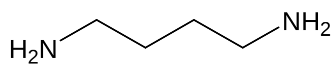
1,5-Diaminopentane $C_5H_{14}N_2$	1,5-Pentanediamine; Cadaverine	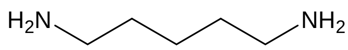
Spermidine $C_7H_{19}N_3$	1,5,10-Triazadecane	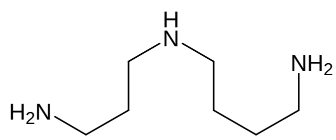
Norspermidine $C_8H_{21}N_3$	Bis(3,3'-aminopropyl)amine	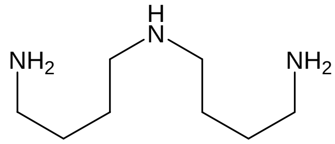
Spermine $C_{10}H_{26}N_4$	N,N'-Bis(3-aminopro pyl)-1,4-diaminobuta ne	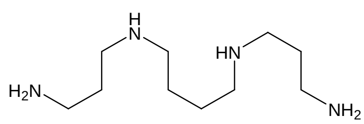

Aromatic amine:

Chemical Name Molecular Formula	Synonyms	Structural Formula
Histamine $C_5H_9N_3$	2-(4-Imidazolyl)ethyl amine	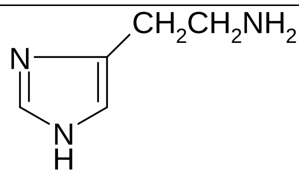
Tryptamine $C_{10}H_{12}N_2$	3-(2-aminoethyl)indole	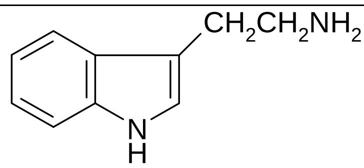
Serotonin $C_{10}H_{12}N_2O$	5-Hydroxytryptamine	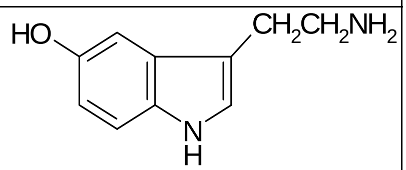
Benzylamine C_7H_9N		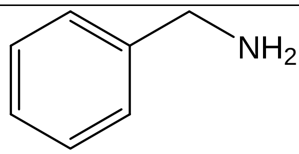
Phenylethylamine $C_8H_{11}N$		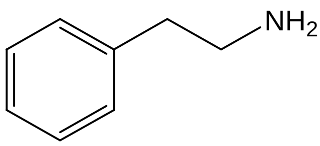

Phenylpropylamine $C_9H_{13}N$		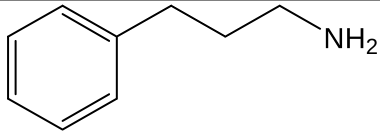
Phenylbutylamine $C_{11}H_{13}N$		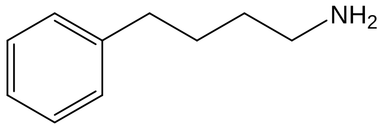
Tyramine $C_8H_{11}NO$	4-(2-Aminoethyl)phenol-4-Hydroxyphenethylamine Tyrosamine	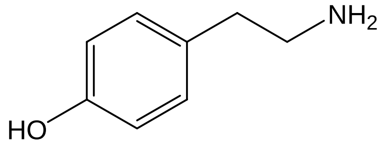
Dopamine $C_8H_{11}NO_2$	3-Hydroxytyramine	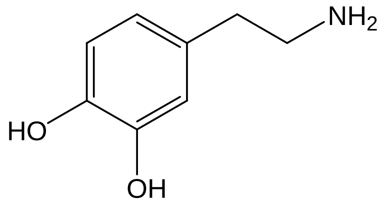
(-)- Noreprinephrine $C_8H_{11}NO_3$	L-Arterenol	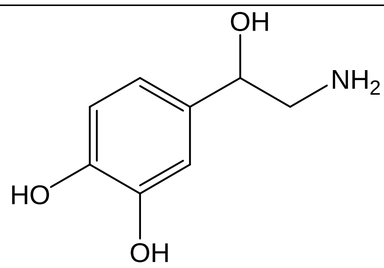

Appendix 5. Plasmids and vectors used in the work

Number	Name	Origin
1	pET30(-S)/AGHO	Chang S. P., 2003
2	pGEM-T easy/ AGHO-reverse	This project
3	pGEM-T easy/ AGHO-reverse (A156D)	This project
4	pGEM-T easy/ AGHO-reverse (A156D/L158W)	This project
5	pGEM-T easy/ AGHO-reverse (A156S/P157G)	This project
6	pGEM-T easy/ AGHO-reverse (A156S/P157G/L158D)	This project
7	pGEM-T easy/ AGHO-reverse (L158D)	This project
8	pET30b(-S)/AGHO (A156D)	This project
9	pET30b(-S)/AGHO (A156D/L158W)	This project
10	pET30b(-S)/AGHO (A156S/P157G)	This project
11	pET30b(-S)/AGHO (A156S/P157G/L158D)	This project
12	pET30b(-S)/AGHO (L158D)	This project

Appendix 6. Primers of site-directed mutagenesis

Primer	Sequence (from 5’ end to 3’ end)
Sequence primer (L)	5:CGGTCCCTCGACGTCCGC:3
Sequence primer (R)	5:GAACCCGACGCGCAGGTC:3
AGHO A156D (L)	5:CAGGTGCGCGTCGACCCCCTCTCGGCG:3
AGHO A156D (R)	5:CGCCGAGAGGGGGTCGACGCGCACCTG:3
AGHO A156D/ L158W (L)	5:GTGCGCGTCGACCCCTGGTCGGCGGGCGTC:3
AGHO A156D/ L158W (L)	5:GACGCCCGCCGACCAGGGGTCGACGCGCAC:3
AGHO A156S/P157G (L)	5:CCGGCACAGGTGCGCGTCTCAGGCCTCTCGGCGGGCGTC:3
AGHO A156S/P157G (R)	5:GACGCCCGCCGAGAGGCCTGAGACGCGCACCTGTGCCGG:3
AGHO A156S/P157G/L158D (L)	5:CGCGTCTCAGGCGACTCGGCGGGCGTCTTC:3
AGHO A156S/P157G/L158D (R)	5:GAAGACGCCCGCCGAGTCGCCTGAGACGCG:3
AGHO L158D (L)	5:CGCGTCGCTCCCGACTCGGCGGGCGTC:3
AGHO L158D (R)	5:GACGCCCGCCGAGTCGGGAGCGACGCG:3

Appendix 7.   Abbreviation of CAOs from different sources

AGHO	*Arthrobacter globiform* Histamine Oxidase
AGPEO	*Arthrobacter globiformi* Phenylethylamine Oxidase
ECAO	*E. coli* Amine Oxidase
KAMO	*Klesiellus aerogenes* Monoamine Oxidase
ASNAO	*Aspergillus niger* Amine Oxidase
HPAO	*Hansenula Polymorpha* metylamine Oxidase
LSAO	*Lentil* Seedling Amine Oxidase
PSAO	*Pea* Seedling Amine Oxidase
BSAO	*Bovine* Serum Amine Oxidase
hVAP-1	*Human* Vascular Adhesion Protein-1
hABP	*Human* Amiloride-Binding Protein

Appendix 8. The multiple sequences alignment from different CAOs

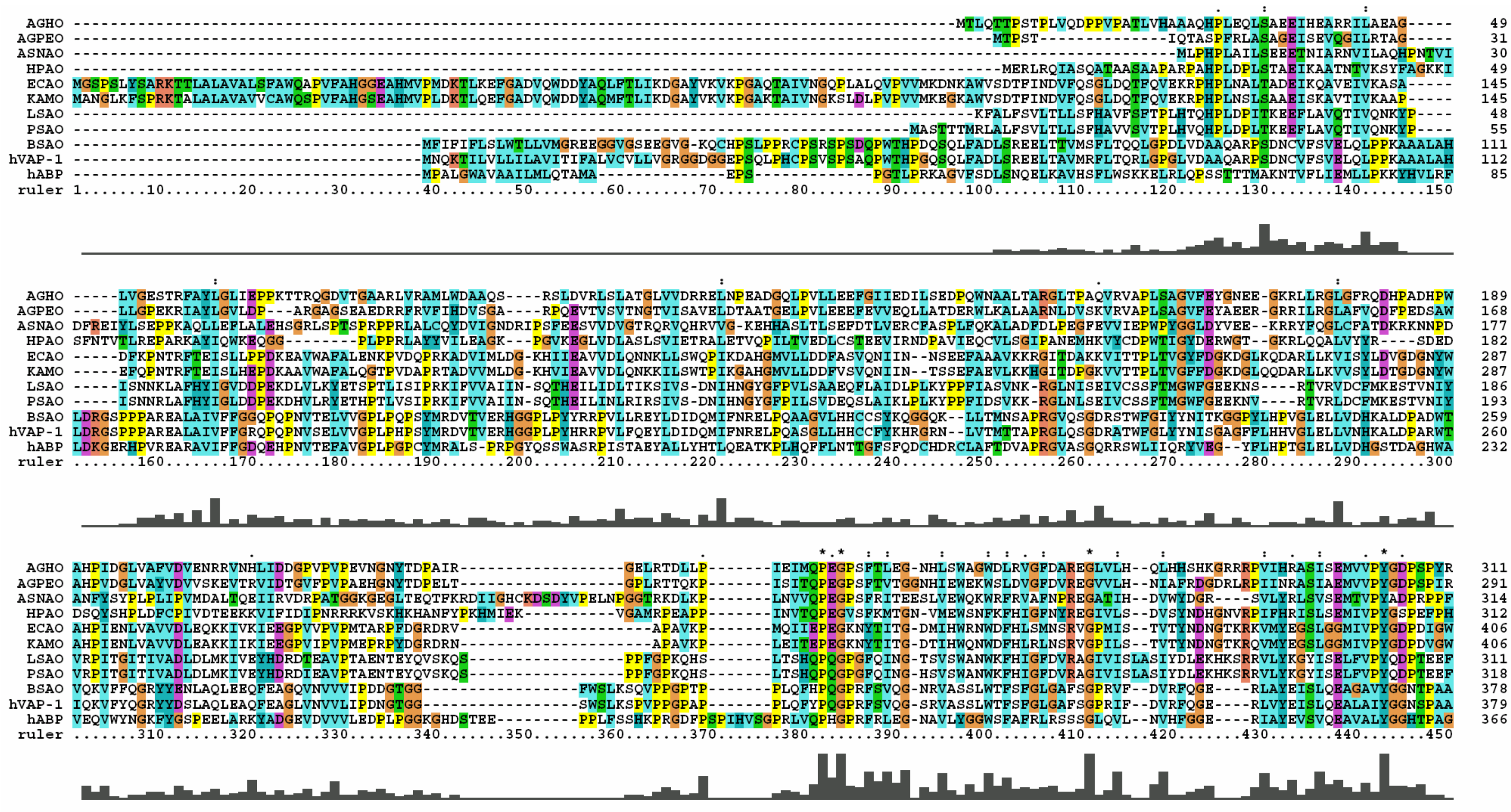

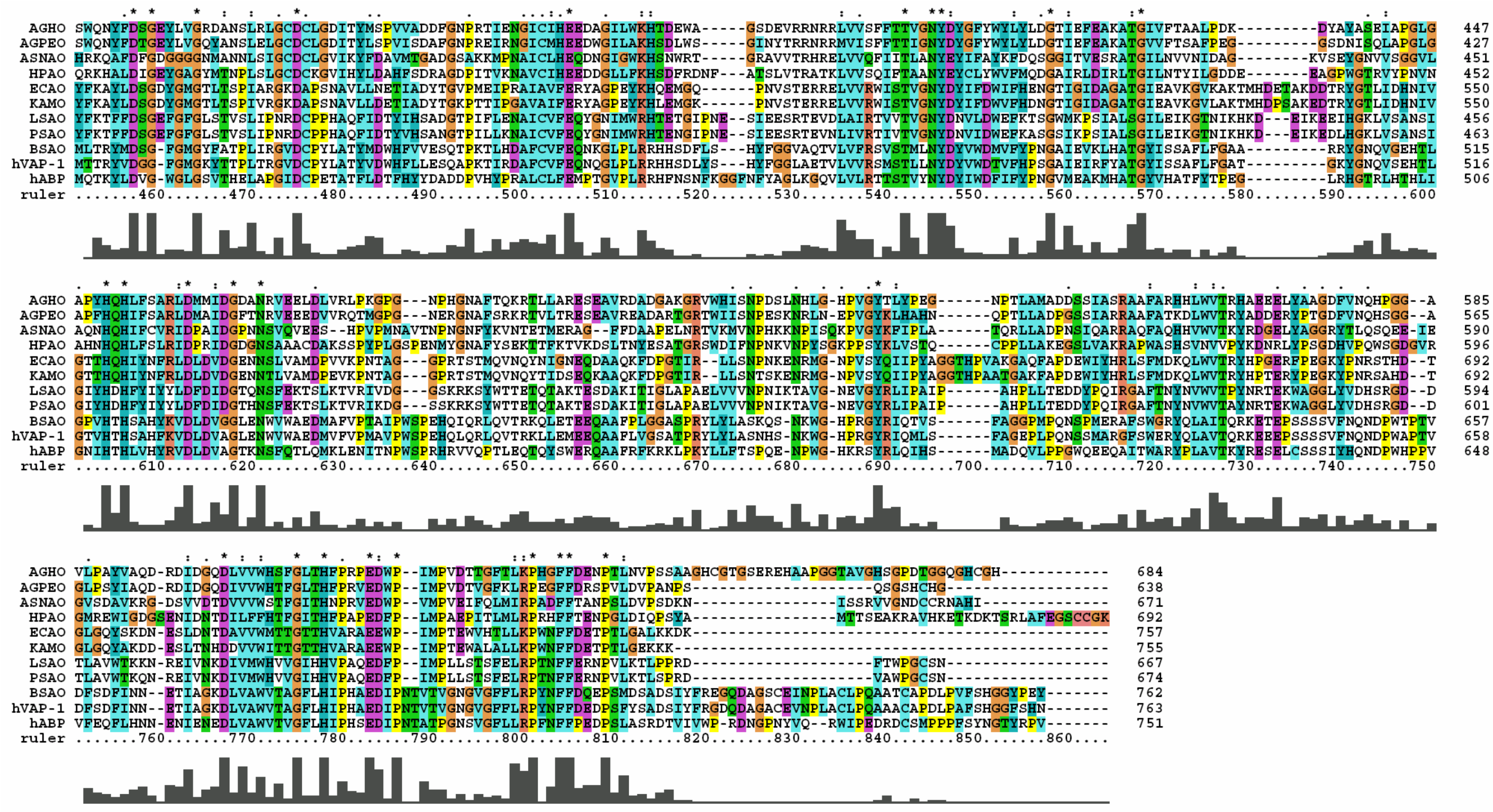

These sequences of different CAOs were aligned by CLUSTAL X (1.81).